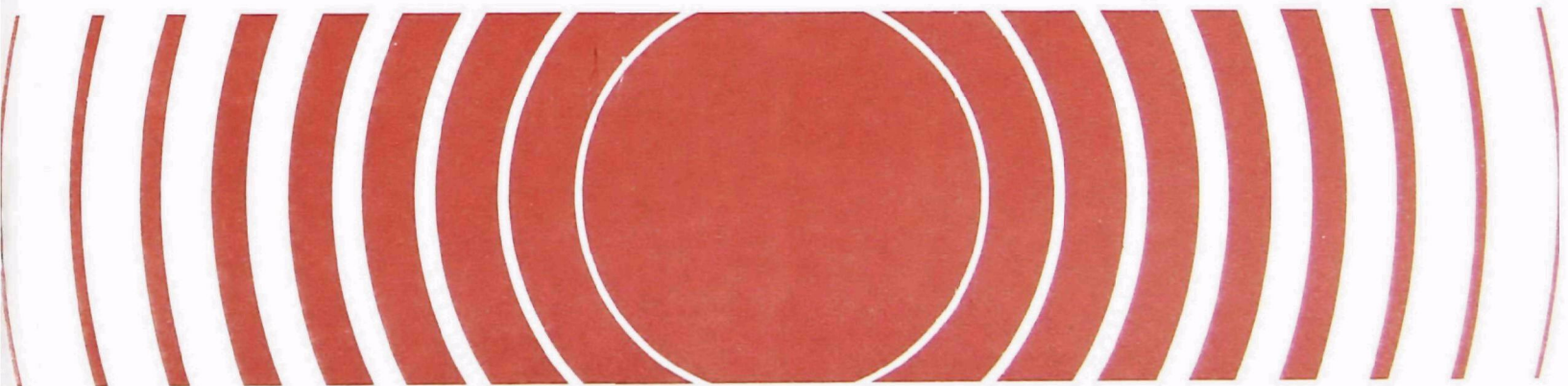


Radiation



A Study of Deep-Ocean Currents Near the 3800 m Low-Level Radioactive Waste Disposal Site May 1984 - May 1986



EPA 520/1-88-007
SAIC - 87/7503/133

A STUDY OF DEEP OCEAN CURRENTS NEAR THE 3800M
LOW-LEVEL RADIOACTIVE WASTE DISPOSAL SITE

May 1984 - May 1986

By
Christopher Casagrande and Peter Hamilton
Science Applications International Corporation
Newport, Rhode Island

Prepared as an account of work sponsored by the
United States Environmental Protection Agency
under Interagency Agreement No. DW14930778-01-0

Project Officer

William R. Curtis

Analysis and Support Division
Office of Radiation Programs (ANR-461)
U.S. Environmental Protection Agency
Washington, D.C. 20460

FOREWORD

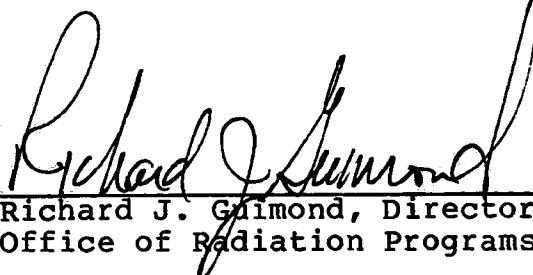
Between 1946 and 1970, the United States disposed of low-level radioactive wastes (LLW) at sites in the Atlantic and Pacific oceans that had been designated for disposal by the former U.S. Atomic Energy Commission.

In 1972 the Congress enacted the Marine Protection, Research, and Sanctuaries Act (Public Law 92-532). This Act charged the Environmental Protection Agency (EPA) with the responsibility to develop criteria and regulations for any ocean disposal of waste materials, including LLW.

In 1974 the EPA Office of Radiation Programs (ORP) initiated studies at previously used LLW disposal sites to determine whether present ocean survey technologies could determine the fate of radioactive wastes disposed in the past. Early studies focused on collecting sediments and marine organisms for radionuclide analyses and evaluating the condition of LLW packages previously disposed on the seafloor. Subsequent studies were conducted to identify pathways and determine mechanisms for potential transport of radionuclides from disposal sites. Sediment resuspension and transport, due to the effects of near-bottom ocean currents, is a potential mechanism for dispersal of radionuclides in the deep-sea. Thus, ORP has studied near-bottom circulation in and near disposal sites to determine the potential for shoreward transport of LLW.

This report presents the results of a study of near-bottom currents at the Atlantic ocean 3800 meter LLW disposal site. Continuous measurements were obtained between 1984 and 1986 at approximately 5, 100, 250, 400 and 1,000 meters above the bottom. The report describes deployments and recoveries of the Aanderra current meters, data return and processing, data analysis, and the potential for sediment transport of radionuclides.

The Agency invites all readers of this report to send any comments or suggestions to Mr. David E. Janes, Director, Analysis and Support Division, Office of Radiation Programs (ANR-461), Environmental Protection Agency, Washington DC, 20460.



Richard J. Guimond, Director
Office of Radiation Programs

PREFACE

This report presents the results of a two-year study of deep ocean currents from May 1984 through May 1986 at the U.S. 3800-m low-level radioactive waste disposal site near the mouth of the Hudson Canyon. The program objectives were to describe the currents, including their source and variability, and deduce from the data the potential for, and direction of, transport of contaminants from the disposal area. The study was accomplished under an interagency agreement between the EPA and the Minerals Management Service (MMS) which combined the disposal area study with the on-going MMS study of physical processes on the Mid-Atlantic slope and rise in order to gain the maximum benefit from a larger data base.

The results show that the currents in the disposal area range in strength from a few to 62 cm sec^{-1} and are principally due to the presence of low frequency topographic Rossby waves having periods of approximately two to four weeks. The currents generally flow towards the southwest, in line with the general topography of the mid-Atlantic region.

The canyon acts to distort the southwest flow, resulting in currents below the canyon rim which are aligned with the canyon onshore-offshore axis. The direction of currents along the canyon axis appears to be determined by the proximity of both the Gulf Stream and the Western Boundary Undercurrent. The currents also exhibit the Rossby wave characteristic of bottom intensification and penetrate to the floor of the Hudson Canyon.

During the study period, several relatively strong current events occurred in up- and down-channel directions of the canyon, with the strongest current (62 cm/sec) directed up-channel (westward). The currents are sufficiently strong to transport dissolved contaminants toward shallower water where they could potentially be entrained by the Western Boundary Undercurrent and transported toward Cape Hatteras. On the other hand, particulate matter that is fine enough to be transported by the relatively strong currents at the disposal site would probably be deposited further up-channel, as the influence of the Rossby wave current amplitudes decrease toward the continental rise. Whether the particles could leave the canyon and reach the middle continental rise would require further study.

This report is organized into five sections, as follows: (I) Introduction; (II) Current Measurement Program; (III) Literature Review; (IV) Data Analysis; and (V) Summary. References are contained in Section VI.

TABLE OF CONTENTS

	<u>Page</u>
FOREWORD	iii
PREFACE	v
LIST OF FIGURES	viii
LIST OF TABLES	xi
I. INTRODUCTION	
1.1. Overview	1
II. CURRENT MEASUREMENT PROGRAM	
2.1 Mooring Design and Instrumentation	6
2.2 Deployment, Rotation and Retrieval Cruises	8
2.3 Data Return	8
2.4 Data Processing	14
III. LITERATURE REVIEW	
3.1 Introduction	16
3.2 The Gulf Stream	17
3.3 Near Bottom Currents	18
IV. DATA ANALYSIS	
4.1 Introduction	24
4.2 Mean Currents	24
4.3 Topographic Rossby Waves (TRWs)	25
4.4 Relationship to the Gulf Stream	37
4.5 Higher Frequency Motions	41
V. SUMMARY	45
VI. REFERENCES	48
VII. ACKNOWLEDGMENTS	51

LIST OF FIGURES

		<u>Page</u>
Figure 1-1	Locations (circles) of the mooring deployments and the 3800-m low-level radioactive waste disposal site superimposed on the bathymetry of the Hudson Canyon (Hanselman and Ryan, 1983).	2
Figure 1-2	Location of the U.S. 3800-m low-level radioactive waste disposal site in relation to the MASAR program moorings.	3
Figure 1-3	Location of the SEEP and Gulf Stream Variability programs affiliated with MASAR/EPA.	4
Figure 2-1	Design of Mooring I deployed at the 3800-m low-level radioactive waste disposal site.	7
Figure 2-2	Time line of the deployment period and the usable data from each instrument at the designated nominal depth.	9
Figure 3-1	Gulf Stream north wall separation distance from the 3 MASAR mooring lines derived from NOAA AAVHRR satellite infrared imagery.	19
Figure 3-2	Map of MASAR study area showing near-bottom mean current vectors from historical and MASAR data.	21
Figure 3-3	A comparison of mean velocities and variance ellipses at 4000 m for the western North Atlantic.	22
Figure 4-1	7-DLP temperatures (top) and currents (bottom) by level on Mooring I.	26
Figure 4-2a	Five month data record beginning May 29, 1984 of 40-HLP of temperatures (top) and currents (bottom) by level on Mooring I at the 3800-m low-level radioactive waste disposal site.	28
Figure 4-2b	Five month data record beginning September 26, 1984 of 40-HLP of temperatures (top) and currents (bottom) by level on Mooring I at the 3800-m low-level radioactive waste disposal site.	29

LIST OF FIGURES (CONT.)

	<u>Page</u>
Figure 4-2c	Five month data record beginning January 1, 1985 of 40-HLP of temperatures (top) and currents (bottom) by level on Mooring I at the 3800-m low-level radioactive waste disposal site. 30
Figure 4-2d	Five month data record beginning April 30, 1985 of 40-HLP of temperatures (top) and currents (bottom) by level on Mooring I at the 3800-m low-level radioactive waste disposal site. 31
Figure 4-2e	Five month data record beginning August 28, 1985 of 40-HLP of temperatures (top) and currents (bottom) by level on Mooring I at the 3800-m low-level radioactive waste disposal site. 32
Figure 4-2f	Five month data record beginning January 1, 1986 of 40-HLP of temperatures (top) and currentss (bottom) by level on Mooring I at the 3800-m low-level radioactive waste disposal site. 33
Figure 4-3	Spectra of (a) kinetic energy for levels I 2 (dashed) and I 4 (solid), and (b) temperature for instrument levels I 2 (solid) and I 5 (dashed). 35
Figure 4-4	Spectra of the (a) U component and (b) V component for I 2 (1 - solid) and I 4 or I 5 (2 - dashed). 36
Figure 4-5	Coherence and phase differences between (a) the U components (1 - solid) and the V components (2 - dashed), with axes rotated 30°, of I 2 and I 4, and (b) the temperature at I 2 and I 4 or I 5. 38
Figure 4-6	Coherence and phase differences between the U (1 - solid) and V (2 - dashed) components, with axes rotated 30°, and the temperature at level (a) I 2 and (b) I 5. 39
Figure 4-7	Rotary spectra for (a) I 1 clockwise component (1 - solid) and anticlockwise component (2 - dashed) and (b) I 4 clockwise component (1 - solid) and anticlockwise component (2 - dashed). 42

LIST OF FIGURES (CONT.)

	<u>Page</u>
Figure 4-8	
(a) Kinetic energy spectra plotted in variance preserving form for I 1 for 171 days beginning November 2, 1985.	43

LIST OF TABLES

		<u>Page</u>
Table 2-1	Aanderaa Current Meter Specifications, Model RCM-5	10
Table 2-2	EPA Cruises To Deploy, Service and Recovery Mooring I Between February 1984 and May 1986.	11
Table 2-3	Location of EPA Mooring I from May 1984 To May 1986.	12
Table 2-4	Overall 2-year EPA Mooring I Instrument Average Data Return By Parameter Measured At Each Level.	13
Table 4-1	40-HLP Statistics for EPA Mooring I	47

I. INTRODUCTION

1.1 Overview

In 1976, the U.S. Environmental Protection Agency (EPA), Office of Radiation Programs, initiated a survey of the Atlantic 3800-m radioactive dumpsite, the approximate center of which is indicated by the triangle shown in Figure 1-1. The objective of this survey was to determine the potential for any possible migration of radioactive materials, dumped between 1957 and 1959, toward shore and/or productive fishing areas. However the determination of currents in the area was not completed. Therefore in March, 1984, the EPA under interagency agreement #DW14930778-01-0 with the Minerals Management Service (MMS) contracted with Science Applications International Corporation (SAIC) to study the currents in and around the 3800-m dumpsite area, as SAIC was already contracted to MMS to study the Mid-Atlantic Slope and Rise (MASAR) dynamics west of the dumpsite to a depth of 3000 m.

This report presents the final results of the two year current measurements effort, from May 1984 to May 1986, in which a single EPA mooring was deployed near the Hudson Canyon to determine the circulation effects on the 3800-m dumpsite. The array was re-deployed four times - in May and October 1984, and April and November 1985. Recovery occurred in May 1986.

The measurement of near-bottom currents at the 3800-m dumpsite was part of the MASAR program. The location of the 3800-m dumpsite current measurement mooring in relation to the MASAR moorings is shown in Figure 1-2.

The MASAR program, as part of the MMS Outer Continental Shelf Environmental Studies (OCS) Program, focused on the following:

- Eddies, rings, streamers, and other Gulf Stream (GS) related events
- The Western Boundary Undercurrent (WBUC)
- Circulation in the surface layer above the main thermocline (less than 200 m)
- The shelf/slope front

To study these dynamical processes, the MASAR principal investigators utilized hydrography, satellite imagery, data from affiliated programs in the area, and Eulerian current measurements.

Several of the MASAR affiliated programs (Fig. 1-3) also supported the dumpsite interpretative effort. These were:

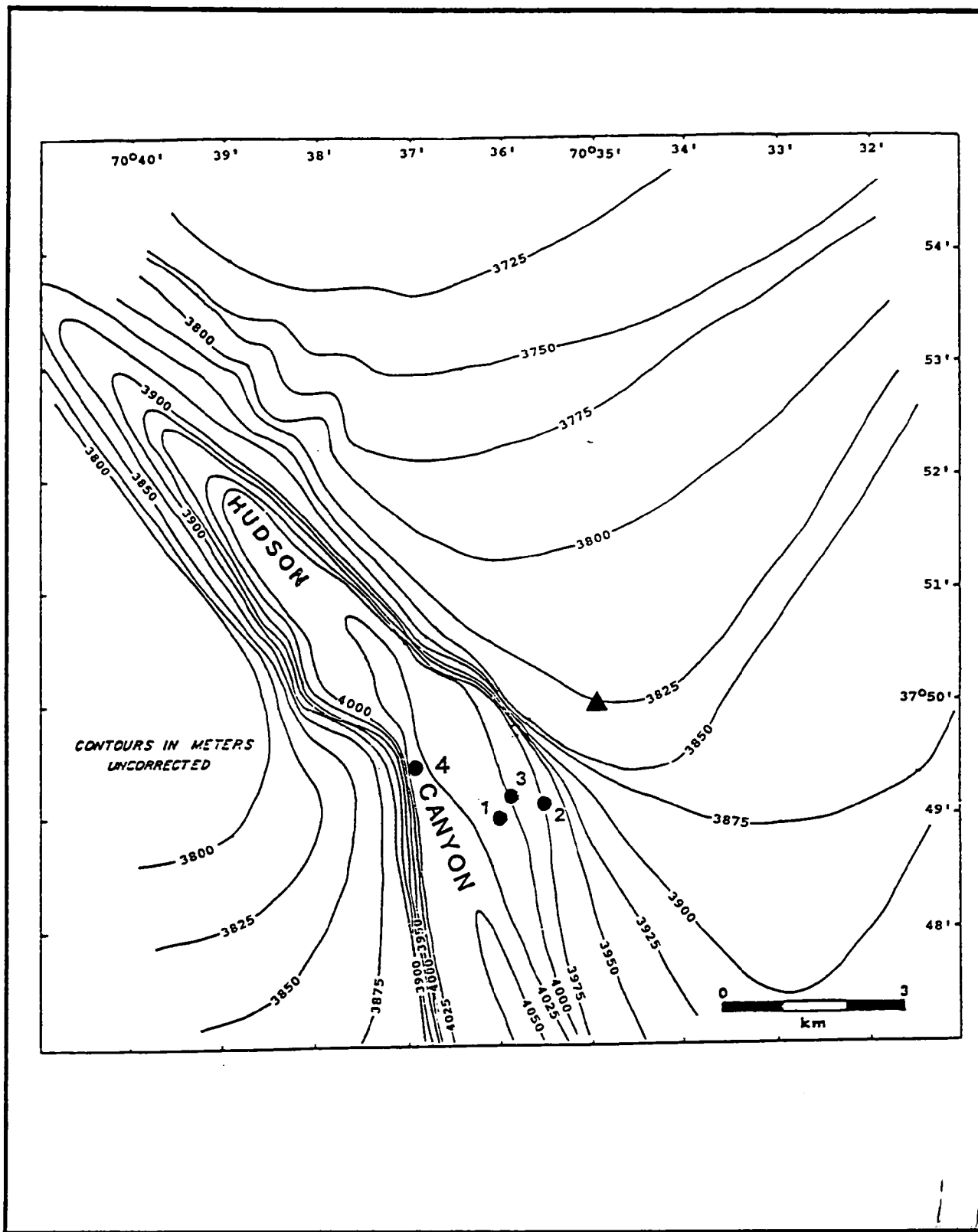


Figure 1-1. Locations (circles) of the mooring deployments and the 3800-m low-level radioactive waste disposal site superimposed on the bathymetry of the Hudson Canyon (Hanselman and Ryan, 1983). Positions 1, 2, 3, and 4 refer to the May and October 1984 and April and November 1985 mooring deployment positions, respectively. The triangle represents the center of the 3800-m disposal site.

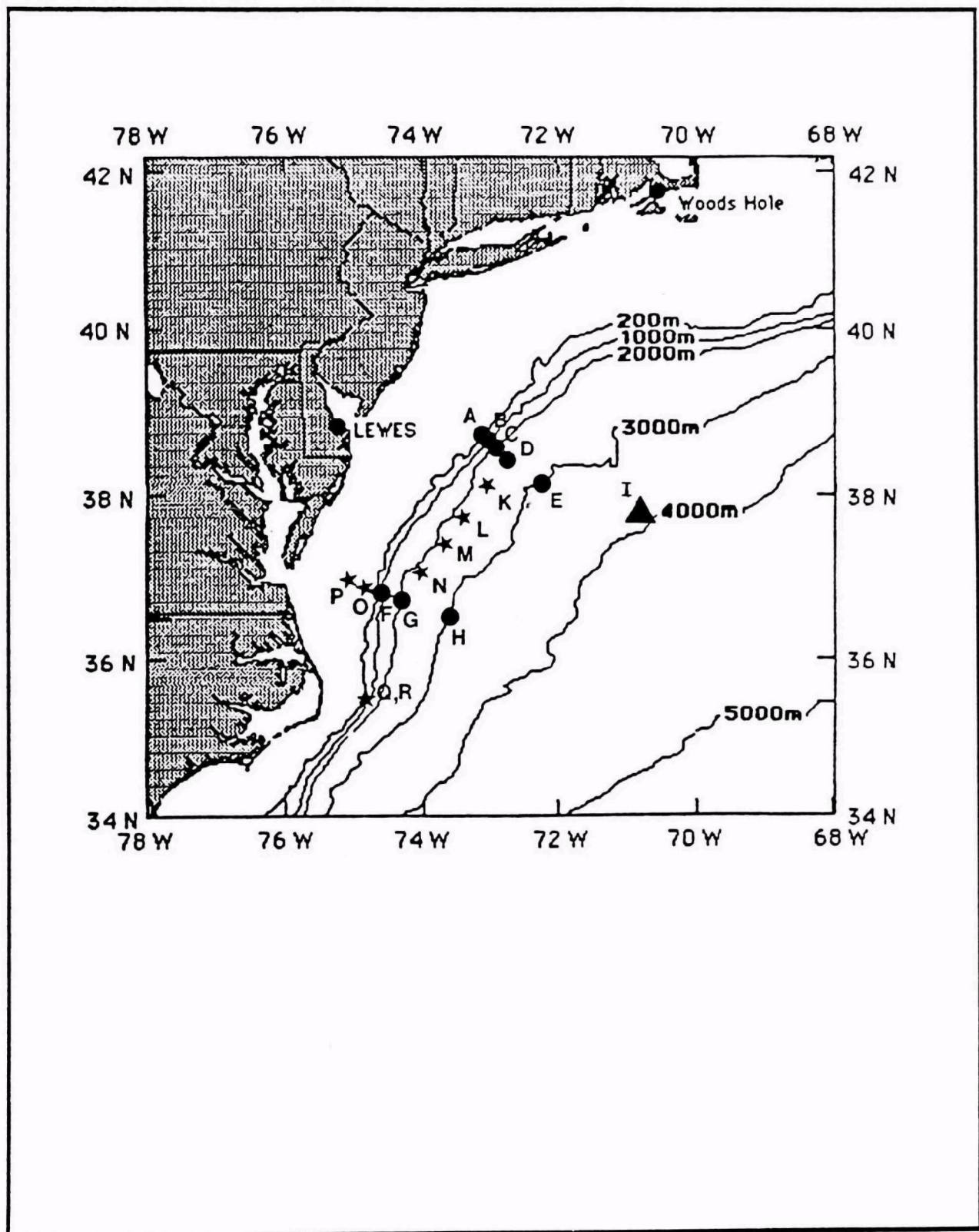


Figure 1-2. Location of the U.S. 3800-m low-level radioactive waste disposal site in relation to the MASAR program moorings. The triangle represents mooring I, at the 3800-m site, initially deployed in May 1984; the circles denote MASAR moorings deployed in February 1984 and the stars those deployed in September 1985.

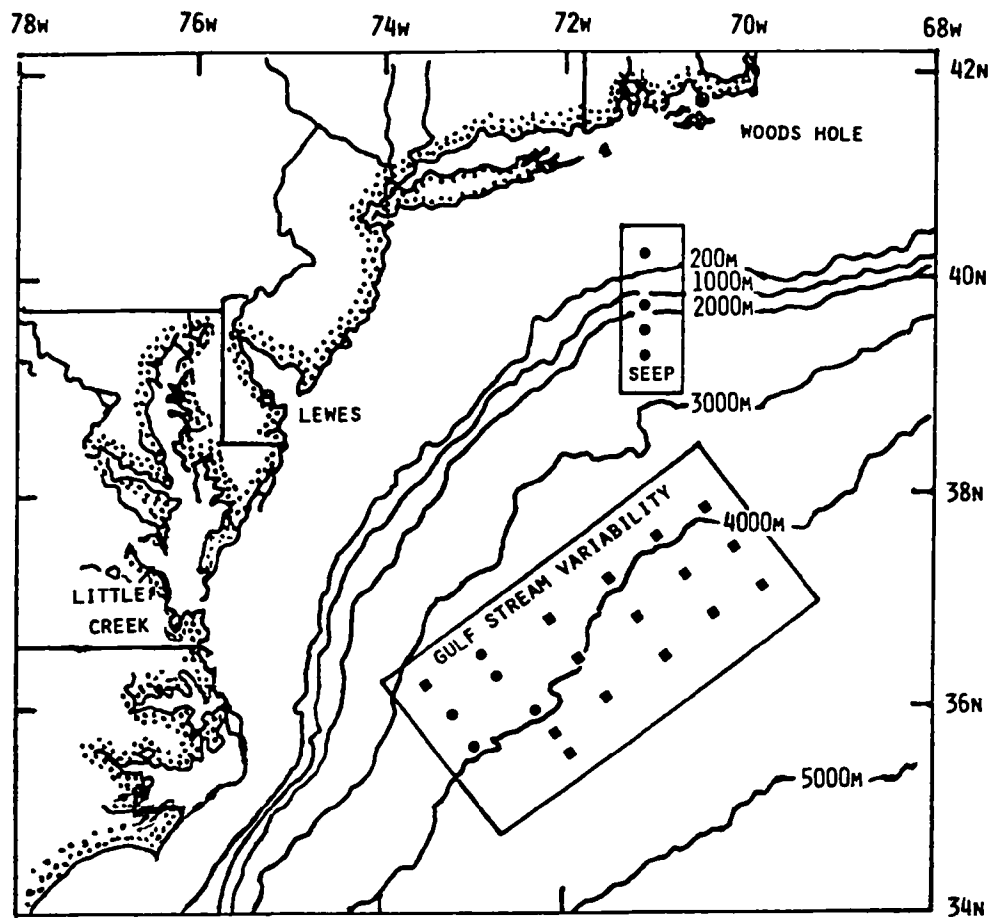


Figure 1-3. Location of the SEEP and Gulf Stream Variability programs affiliated with MASAR/EPA. Circles represent current meter moorings, boxes represent locations of Inverted Echo Sounders (IES).

- The Warm-Core Rings Experiment (WCRE), funded by NSF and conducted by the Rosenstiel School of Marine and Atmospheric Science (RSMAS). The satellite infrared imagery part of the program, provided much of the 10 year statistical information on Warm-Core Rings (WCRs) used in this report.
- The Gulf Stream Meander Dynamics Program, sponsored by the National Science Foundation (NSF) and the Office of Naval Research (ONR). This program was designed to study the meandering processes of the Gulf Stream (GS).
- The Shelf-Edge Exchange Processes (SEEP), a program supported by the Department of Energy (DOE). The program's objectives were to describe and quantify the cross-shelf transport and subsequent deposition on the slope of organic carbon.

II. CURRENT MEASUREMENT PROGRAM

2.1 Mooring Design and Instrumentation

2.1.1 Mooring Design

One of the major requirements of a successful mooring design is that the instruments attached to the mooring remain within a predetermined depth range when subjected to environmental conditions. The first step in the design process is to estimate the range of current speeds expected at the deployment sites.

Three velocity profiles (speed vs. depth) representing low, mean, and high speed, were generated from historical data. The mean speed profile was used to determine the initial mooring design and the high and low profiles were applied to that design as a check on potential vertical instrument excursions and mooring tilt at the instrument attachment points.

Next, the mooring design was configured with the instruments at their required depth and the mooring assumed to be completely vertical. Sufficient flotation was calculated and configured to maintain a positive tension in the supporting cable; a simple summing of submerged weights provided the amount of tension. A safety factor of two, between working and yield strengths, was used for this mooring design.

The preliminary design was then subjected to SAIC's Static Buoy Analysis Computer Program (SBAP). The program computes the shape of the mooring cable when subjected to expected ocean current forces. Confirmation of the computer design was later analyzed by comparing the initial design with the actual mooring performance.

The final design used at the 3800-m dumpsite is shown in Figure 2-1. Attached to the mooring were five Aanderaa RCM-5 current meters. The meters were nominally spaced to be approximately 5, 100, 250, 400, and 1000 m above the ocean floor. The spacing was designed to allow comparison of currents above, at, and below the Hudson canyon rim. The lower two instruments were in the canyon, the third approximately level with the rim, and the upper two situated approximately 100 and 700 m above the rim.

The required flotation to maintain the mooring upright was distributed along the entire mooring length. In case of severance at some point along the mooring array, the distribution of flotation would insure that the remaining portion functioned normally and would rise to the surface when released by command.

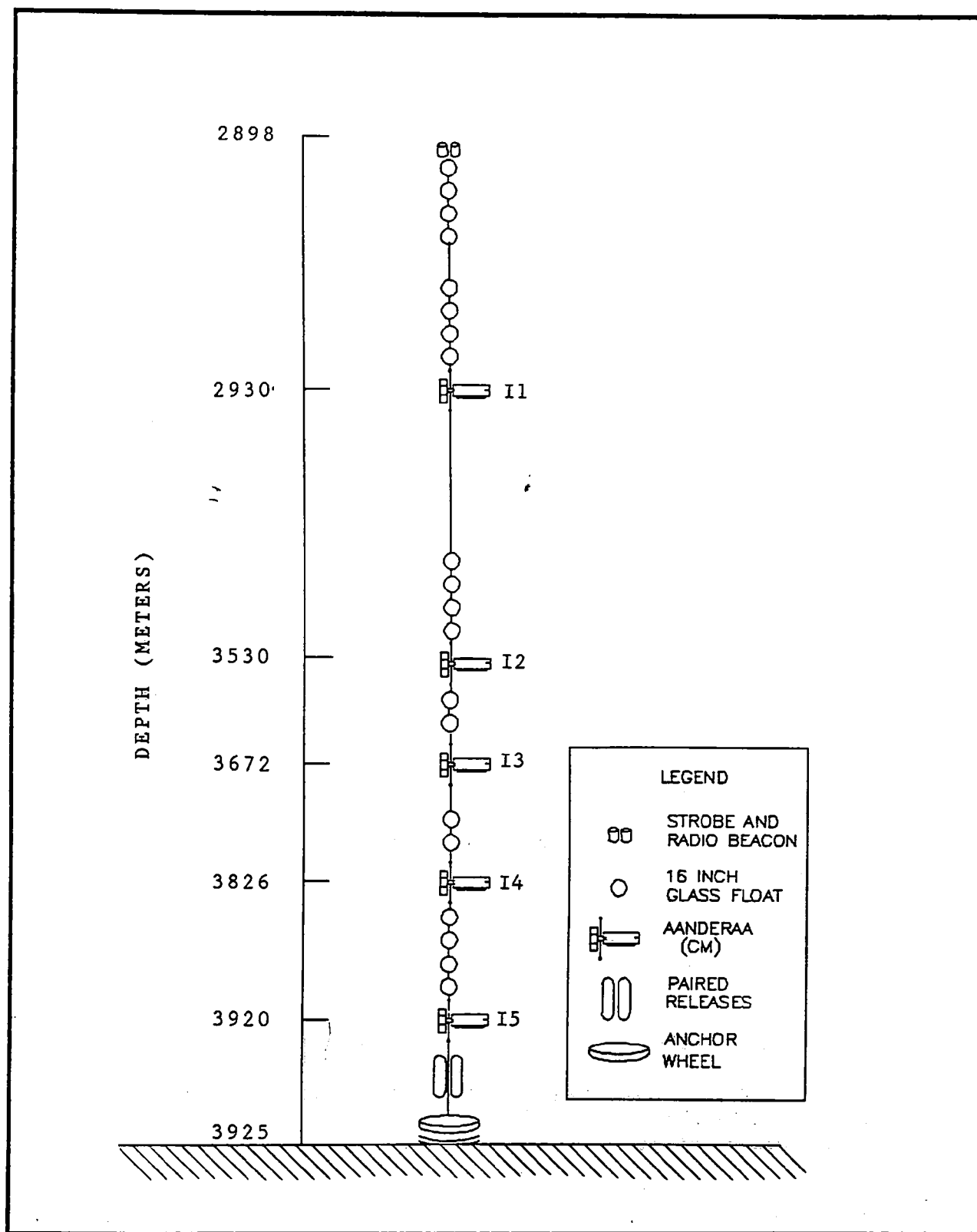


Figure 2-1. Design of Mooring I deployed at the 3800-m low-level radioactive waste disposal site.

2.1.2 Instrumentation

The five Aanderaa RCM-5 current meters used on the mooring were supplied by EPA as government furnished equipment (GFE). After twelve months of field use they were replaced by newly calibrated RCM-5 current meters (also GFE). All current meters were calibrated before and after deployments in order to minimize data error.

These meters are intended for use in deep ocean waters below the wave zone, are self-contained and record current speed, direction, temperature, and other parameters as configured by the user.

Each current meter was attached to a swivel and shaft assembly mounted in-line with other mooring components. The current speed was measured by a rotor. Revolutions were counted and averaged, and then recorded on magnetic tape along with current direction from a magnetic compass and water temperature from a thermistor. Specifications for the Aanderaa current meters are given in Table 2-1.

2.2 Deployment, Rotation, and Retrieval Cruises

During the two-year study there were five cruises to deploy, service, and recover the EPA Mooring designated as "I". The cruise dates, ships used and ports are shown in Table 2-2.

Figure 1-1 shows the position of mooring "I" near the northeast side of the canyon after each deployment. The exact locations, determined from Loran-C navigation, are given in Table 2-3. The first three deployments were within 500 - 600 m of each other. The fourth deployment was situated along the southwest canyon wall to better define in-canyon circulation. Although each mooring was identical in design, the differences in total water depth for each location resulted in different instrument depths.

2.3 Data Return

Total usable data, from each instrument level, are shown in Table 2-4. A time line of deployment periods and data obtained at each instrument level is shown in Figure 2-2. The lowest semiannual data return occurred during the first 6-month deployment when older-designed current meters were used, resulting in a variety of failures. One meter flooded because of transducer failure. Another meter experienced compass failure associated with in-situ low temperatures. The compass functioned normally before and after deployment. A third meter's battery failed. During the second deployment period, the top meter

Figure 2-2. Time line of the deployment period and the usable data from each instrument at the designated nominal depth.

Table 2-1. Aanderaa Current Meter Specifications, Model RCM-5.

Current Speed	Sensor: Rotor with magnetic coupling Output: Revolutions counted electronically Threshold: 2.5 cm/s Maximum: 250 cm/s
Current Direction	Compass: Magnetic; coupled to external vane assembly Resolution: 0.35 degree Accuracy: 7.5 degrees
Temperature	Sensor: Thermistor Resolution: 0.1% of range Accuracy: 0.05 degree C
Time Base	Source: Quartz Accuracy: 2 sec/day
Data Storage	600 feet of 1/4 inch reel to reel magnetic tape Capacity: 10,000 readings
Mechanical	Housing: Cu Ni Si alloy, epoxy coated Depth: 6000 meters Weight: 26.6 kg in air 17.3 kg in water
Sampling	Interval: 30 sec - 180 min Modes: one

Table 2-2. EPA Cruises To Deploy, Service and Recovery Mooring I Between February 1984 And May 1986.

SHIP	DATES	PORT(S)
U. of Del. vessel Cape Henlopen	27 - 31 May 1984	Lewes, DE
NOAA vessel Mt. Mitchell	26 - 28 October 1984	Sandy Hook, NJ to Shinnecock, NY
NOAA vessel Atlantis IV	29 April - 1 May 1985	WHOI
SAIC contract vessel Seaward Explorer	29 Oct. - 11 Nov. 1985	Morehead City, NC to Norfolk, VA
EPA vessel Peter W. Anderson	5 - 10 May 1986	Little Creek, VA to Balitimore, MD

Table 2-3. Location Of EPA Mooring I From May 1984 To
May 1986.

Deployment		Location	Loran	*	*
No.	Date	Coordinates	TD	Water Depth	Moor Top
=====					
1	5/31-10/28/84	37°49.2'N 70°36.2'W	25723.6 42292.6	3925 m	2898 m
2	10/28/84-5/1/85	37°49.3'N 70°35.7'W	25721.4 42293.8	3905 m	2879 m
3	5/1-11/11/85	37°49.2'N 70°35.9'W	25722.7 42294.2	3922 m	2895 m
4	11/11/85-5/10/86	37°49.5'N 70°37.1'W	25723.5 42294.0	3922 m	2895 m

*NOTE: Slight variation in total water depth following each deployment results in instrument depths.

Table 2-4. Overall 2-year EPA Mooring I Instrument Average Data Return By Parameter Measured At Each Level.

Instrument	Nominal Depth Level	Current Speed & Direction	Temperature
I1	2930 m	51%	51%
I2	3530 m	75%	75%
I3	3672 m	69%	69%
I4	3826 m	75%	93%
I5	3920 m	76%	75%

flooded because the input/output port design (this port is used during the pre-development check of the current meter to verify proper operation) did not use an o-ring; later designs corrected this problem. This first group of meters was replaced with a second group of newer meters during the 12th month turnaround. Subsequently, the overall data return for all meters increased from about 58% to better than 80%.

2.4 Data Processing

The data from the four deployments were generally of good quality with the exceptions noted below. After transcription to nine-track computer tape, the velocity and temperature time series were processed and checked for bad data points using established techniques discussed in SAIC (1987). The time series were merged together by interpolating through the gaps caused by the rotation of the mooring at 6 month intervals. The data were then filtered by a three-hour low pass (3-HLP) Lanczos kernel decimating to intervals of 1 hour, a forty-hour low pass (40-HLP) Lanczos kernel decimating to 6-hourly intervals and a 7-day low pass (7-DLP) Lanczos squared kernel decimating to 1 day intervals. The latter filter was used to remove energy at periods less than 7 days so that low frequency Topographic Rossby Wave (TRW) motions could be presented on two-year axes. The majority of Rossby wave energy is at periods longer than 7 days (Thompson, 1977; Hamilton, 1984). This 7-DLP filter was also used extensively in the analysis of the MASAR data.

The current vector time series (see Figs. 4-2a to -2f in Section 4) were plotted with the axes rotated such that the V-component was directed along 030°T and the orthogonal U-component along 120°T. Rotated axes are designated in the data record identification label as "R" for rotation along with the adjacent number "30" designating the degree of rotation, for all direction data in this report. Axes rotation has resulted in the V-component being approximately parallel to the general trend of the isobaths on the continental rise NE and SW of the Hudson canyon and the U-component being in-line with the canyon axis.

The data recovered from instrument level I 4 in the first and second deployments was only partially complete. The low temperatures of the deep ocean caused the compass to seize in this instrument and only a speed record was obtained. For the first and second deployment periods the record was reconstructed by combining the direction from the nearest instrument level, I 3, and I 5 when that at level I 3 malfunctioned, with the speed record from level I 4. This analysis procedure has been shown to produce a good approximation of direction in the presence of low frequency planetary wave motions which are essentially columnar. The results are shown in Figures 4-2a to -2c (Section 4). Directions so constructed for level I 4 should not be used for relatively high frequency inertial or tidal motions since there may be large changes with depth. Thus only the low frequency

data for the first two deployments of I 4 are used in the data analysis section (Section 4) of this report. The columnar motion at low frequencies was checked using data from deployments 3 and 4 with the result that the phase differences through the depth array were not significantly different from zero.

A second problem with the data concerned the calibration of the temperature data for deployments 1 and 2. The temperature sensors for deployments 3 and 4 were calibrated by Lamont Doherty Geological Observatory and SAIC and are considered accurate to the precision of the instrument. Deployments 1 and 2 used old GFE instruments which evidenced calibration drifts. There were differences in mean temperatures between the first and second year deployments, but variances were similar. Therefore, temperature records from deployments 1 and 2 were post calibrated by comparing the temperatures recorded by the older GFE instruments at the end of deployment 2 to those recorded by the newer replacement instruments at the beginning of deployment 3 since the recovery and redeployment time difference was only a few hours. After this correction, the mean temperature profile for the first year was very similar to that for the second year, differing by about 0.02°C at maximum.

III. LITERATURE REVIEW

3.1 Introduction

A review of the oceanography of the Mid Atlantic continental rise was conducted as part of a previous study into the deep currents at the 3800-m low-level radioactive waste dumpsite (Hamilton, 1982). Major experimental studies up to 1981 were reviewed and discussed. This review is basically an updating of the information in Hamilton (1982) and the reader is referred to that document for background material. The 3800-m dumpsite is about 50 km north of the mean historical position of the north wall of the Gulf Stream at 71°W and therefore the Gulf Stream proper generally dominates the upper part of the water column above the main thermocline. The Gulf Stream and related warm- and cold-core rings have been the subject of a number of studies in the last five years.

Earlier current measurements on the continental rise of the Mid-Atlantic Bight have shown that low frequency motions are dominated by topographic Rossby waves (TRW) (Thompson, 1977; Hogg, 1981; Hamilton, 1984). These are planetary wave motions, with periods ranging from about a week to several months, which are characterized by bottom intensification (i.e. current amplitudes increase in magnitude with depth); columnar motions (i.e. zero phase difference between currents at different depths at any particular wave frequency) and the direction of propagation is such that shallow water is on the right (i.e. to the west at the 3800-m site). Horizontal wavelengths are of order 100-200 km and TRWs in the Mid-Atlantic Bight show direction of energy propagation consistent with generation by the Gulf Stream (GS) (Hogg, 1981). The dynamics of TRW generation by the meandering GS are not yet well understood.

Mean near-bottom flows on the continental rise show a consistent westward and southwestward drift following the isobath towards Cape Hatteras. This is known as the Western Boundary Undercurrent (WBUC) and recent measurements from the MASAR and POLYMODE programs are discussed below.

The Gulf Stream leaves the continental margin and flows into deep water at Cape Hatteras, where it becomes a free flowing meandering jet. Time-dependent wavelike, lateral displacements or meanders of the GS are observed along its entire path. Northeast of Cape Hatteras, these meanders show considerable range of periodicities (4-100 days are dominant), wavelengths (200-600 km) and phase speeds (5-40 km d⁻¹). The dominant meanders also grow downstream of Hatteras with a tendency to exhibit a lengthening of period and a decrease in phase speed. By convention, a meander crest (trough) is defined to be the extreme shoreward or northwards (seaward or southwards) displacement of a downstream propagating meander.

3.2 The Gulf Stream

Recent studies of the Gulf Stream have involved the extensive use of SOFAR floats (Richardson et al., 1981; Schmitz et al., 1981; Owens, 1984; Shaw and Rossby, 1984). SOFAR floats follow motions on surfaces of equal pressure (i.e., they are isobaric floats) and thus are not true followers of water particles. New developments in float technology have produced floats that more readily follow water particles on constant density surfaces (Rossby et al., 1985a). These are known as "Rafos" floats and some preliminary results from these devices placed in the Gulf Stream off Cape Hatteras have been reported (Rossby et al., 1985b). A number of Rafos float tracks released at a nominal depth of 500 m (corresponding to about 27 sigma-t) in the GS off Cape Hatteras have remained within the stream for distances of over 2000 km. Only a few transferences of floats into slope water to the north of the GS front occurred. The implication is that at thermocline depths, the GS is an effective barrier to transfer of Sargasso Sea water into slope water. A similar conclusion was arrived from an isopycnal water mass analysis of Gulf Stream 60 hydrographic sections by Bower et al., (1985).

Shaw and Rossby (1984), using SOFAR floats, discuss GS trajectories above and below the thermocline. Using only portions of the float tracks that correspond to GS water masses, they showed that the shallow 700-m level trajectories remained within the GS and between Cape Hatteras and the New England Sea Mounts (approximately 59°W). Thus fluid particles above the main thermocline are advected along with the current over distances comparable to the downstream scale of the current (i.e., the distance between meander crests). A comparison of the deep SOFAR float trajectories (1300 and 2000 m) with the shallow ones showed that a continuous current does not exist below the stream. However the deep floats do show intermittent eastward flow related to the surface current but it is apparent that water parcels below the thermocline can escape from the stream both northward and southward anywhere along its path. The intermittent deep GS may be formed by the acceleration of the shallow stream east of Cape Hatteras. Shaw and Rossby (1984) also provide direct evidence that large meanders and the formation of warm- and cold-core rings can be a direct influence on the 1300-2000-m currents. This adds substance to the ideas that the meandering GS is the source of energy for the ubiquitous Topographic Rossby Wave motions found in the slope region (Luyten, 1977; Hamilton, 1984).

Gulf Stream meanders have been studied from AVHRR thermal imagery (Halliwell and Mooers, 1983; Cornillon, 1986) and from data provided by an array of bottom mounted inverse echo sounders (IES) to sense the position of the main thermocline and thus infer the position of the GS front (Watts and Johns, 1982; Tracey and Watts, 1986). The standard deviation of the envelope of GS frontal positions increases linearly from Cape Hatteras to

71°W. There is a relative minimum at about 69°W followed by about a two-fold increase in the width envelope which then remains relatively constant (standard deviation approximately 80 km) between 68° and 58°W (Cornillon, 1986).

Meander propagation speeds and wavelengths vary considerably. Halliwell and Mooers (1983) found, from an EOF analyses of GS frontal maps, that there were two dominant meander paths downstream of Cape Hatteras. At periods greater than four months the first meander mode was a standing wave with nodes at Cape Hatteras and about at 38°N, 68°W. This accounts for the relative minimum in the GS path statistics found by Cornillon (1986) and others. The second mode resulted from downstream propagating meanders with periods of a few weeks to a few months. The dominant wavelength and period averaged about 330 km and 45 days, respectively. Phase speed was about 8 cm sec⁻¹ with some amplitudes exceeding 200 km. These meanders exhibited a wide range of wavelengths, periods and propagation speeds, while undergoing exponential growth in the first 900 km downstream of Cape Hatteras.

Halliwell and Mooers (1983) showed that there was a weak seasonal dependency in the path of the stream. Tracey and Watts (1986), using IES data showed that the stream tended to be displaced southward in winter which is also the period of highest transport. Recently, Fu et al. (1987) showed the seasonal variation in sea-level difference across the GS front in the Mid-Atlantic from satellite altimeter data, which showed a good correlation with the seasonal variation in large-scale wind/stress curl (with a three month lag). The intense winter cooling over the northwestern Atlantic also plays a role in the intensification of the transport. However the MASAR study showed there is a great deal of inter-annual variability in the path of the stream. For most of the 1984-1985 MASAR period the GS was displaced north of its mean position. This is illustrated by Figure 3-1 (SAIC, 1987) which shows the distance from the shelf break along the MASAR mooring transect (north, south and a transect midway between) of the mean monthly position of GS front. Large amplitude fluctuations are shown in 1982-1984 which were not present in 1985 when the stream was closer, on average, to the slope.

3.3 Near Bottom Currents

Near bottom flows have been generally studied with current meters. Hendry (1982) discusses records from a zonal array of 4 moorings along 40°30'N between 56° and 55°W. The instruments were 1000 m off the bottom in 5000-m water depth. The mean flows were westward along the isobaths and were similar to the westward mean flows measured along 70°W in water depths of less than 4000 m (Luyten, 1977). The westward deep mean flow at 55°W is probably part of the Western Boundary Undercurrent which is observed on the upper continental rise as far as Cape Hatteras. It was more difficult to relate the current

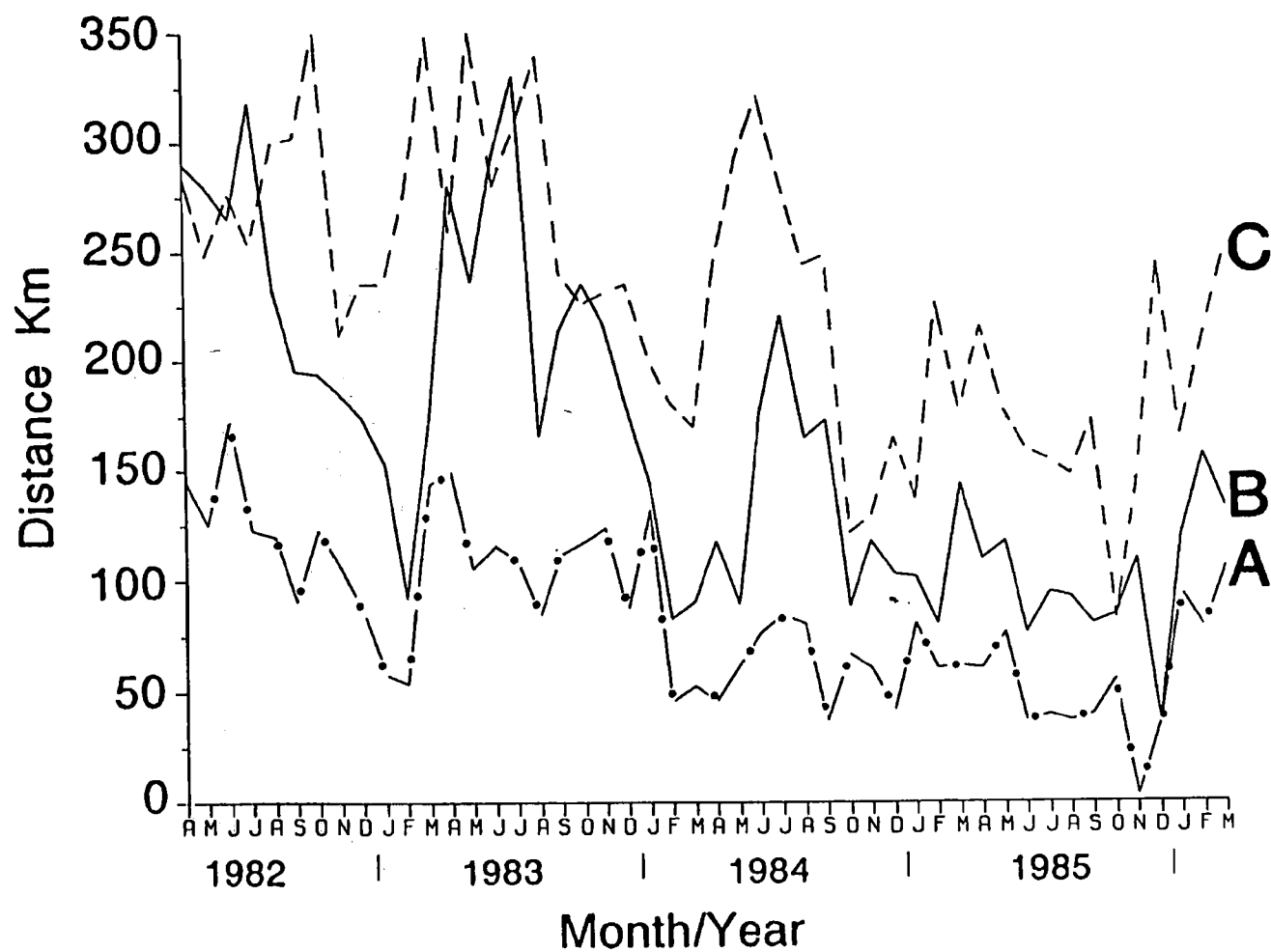


Figure 3-1. Gulf Stream north wall separation distance from the 3 MASAR mooring lines derived from NOAA AVHRR satellite infrared imagery. A, B, C refer to separations from the south, middle and north lines, respectively. (from SAIC, 1987)

fluctuations to GS meanders as has been done intermittently with deep float trajectories (Owens, 1984). Some of the temperature perturbations at these sites could be from Gulf Stream displacements or from the formation of cold- and warm-core rings.

Observations of near bottom currents west of 70°W have been considerably increased by the MASAR experiment (SAIC, 1987). Thus, mean flows upstream and downstream of the low-level radioactive waste sites have some degree of documentation. Figure 3-2 shows the mean currents derived from near bottom current meters (generally 100 - 500 m off the seafloor) from the MASAR experiment (SAIC, 1987); the SEEP experiment (Aikman et al., 1987); the Rise Array experiment along 70°W and 69°30'W (Luyten, 1977); near bottom measurements along 36°N on four moorings in water depths from 1600 to 3700 m off Cape Hatteras (Casagrande, 1983); records 500 and 1000 m off the bottom from five current meters moored under the GS off Cape Hatteras (Johns and Watts, 1986); five 12-month long current meter records at 500 m and 1000 m off the bottom in the same deep GS region (Bane and Watts, 1985); the EPA 2800-m dumpsite (the mean of four near-bottom four month current records is shown, Hamilton (1982)); and finally one additional record from Richardson's (1977) study of the Western Boundary Undercurrent southeast of Cape Hatteras is included. Although this latter record is only two months long, it was 100 m off the bottom in 2600-m water depth, apparently in the core of the WBUC.

The currents are sufficiently consistent to suggest that the estimates of the mean are statistically significant. The resulting pattern suggests that the strongest mean flows are at the base of the continental slope. However, there is also a region between the 3000 and 4000-m isobaths in the vicinity of 70°-72°W where the westward along-isobath flow is relatively stronger than in the middle of the rise. This region is just north of the mean position of the GS front. Mean flows under the GS (MASAR site H and the Rise Array deeper than 4000 m) tend to be negligible or much more variable in direction with perhaps a northward trend.

Figure 3-3 (Fofonoff and Hendry, 1985) shows the low frequency variance ellipses of deep currents, near bottom or 4000 m whichever is shallower, superimposed on Richardson's (1983) surface drifter trajectories. The primary data used came from the Rise Array (Luyten, 1977), the Polymode Local Dynamics Experiment (Owens et al., 1982), and the Polymode Arrays 1 and 2 (Schmitz, 1976; 1980). At 55°W the kinetic energy (proportional to the area of the variance ellipses) is clearly greatest under the GS. There is a marked decrease in variance to the east at approximately 45°W and south to 32°N, and to a lesser degree to the west at 70°W. There is also a tendency towards increasing ellipticity of the variance ellipses to the north of the GS as stronger bottom slopes are encountered on the continental rise.

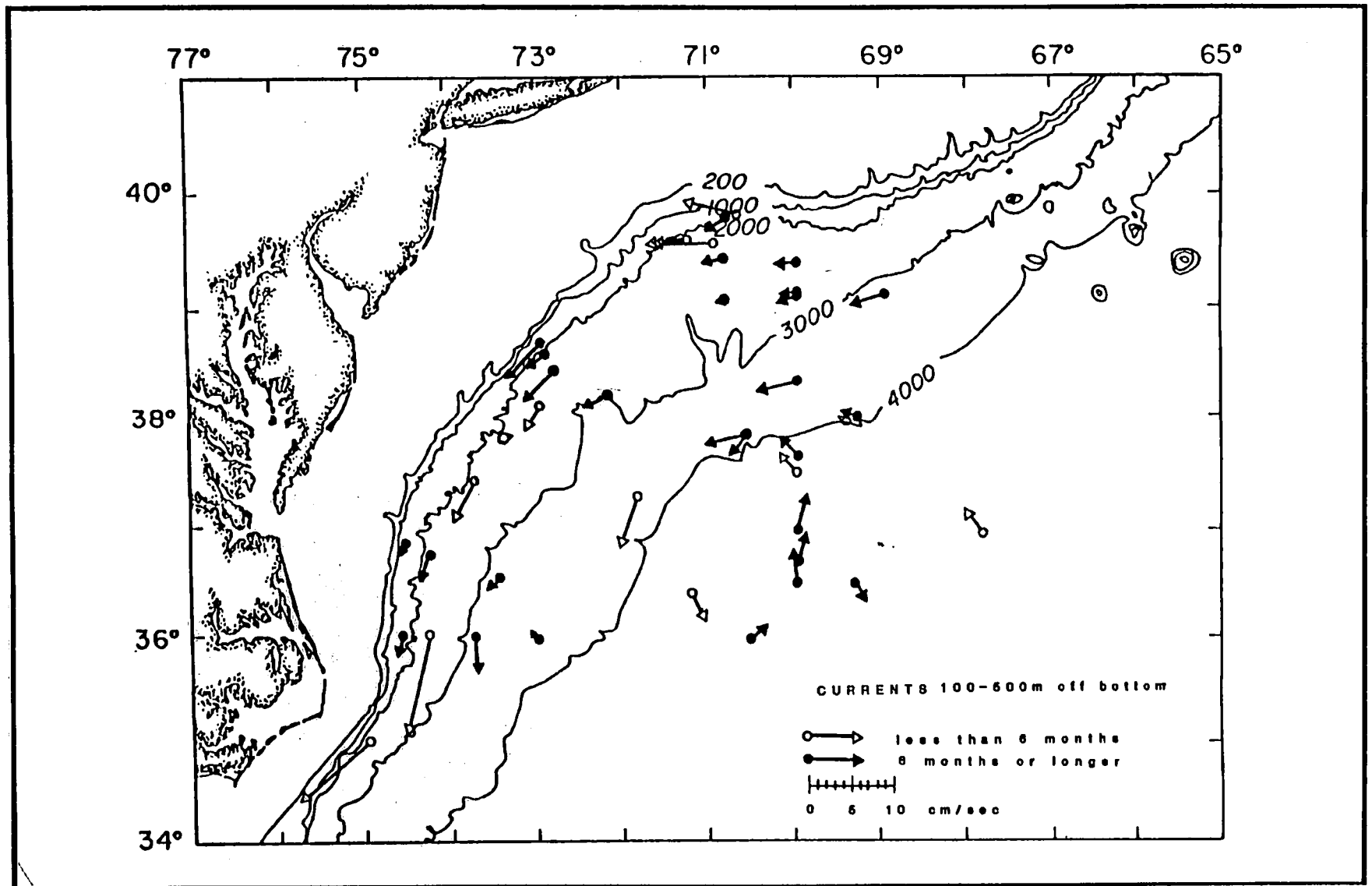


Figure 3-2. Map of MASAR study area showing near-bottom mean current vectors from historical and MASAR data. (from SAIC, 1987)

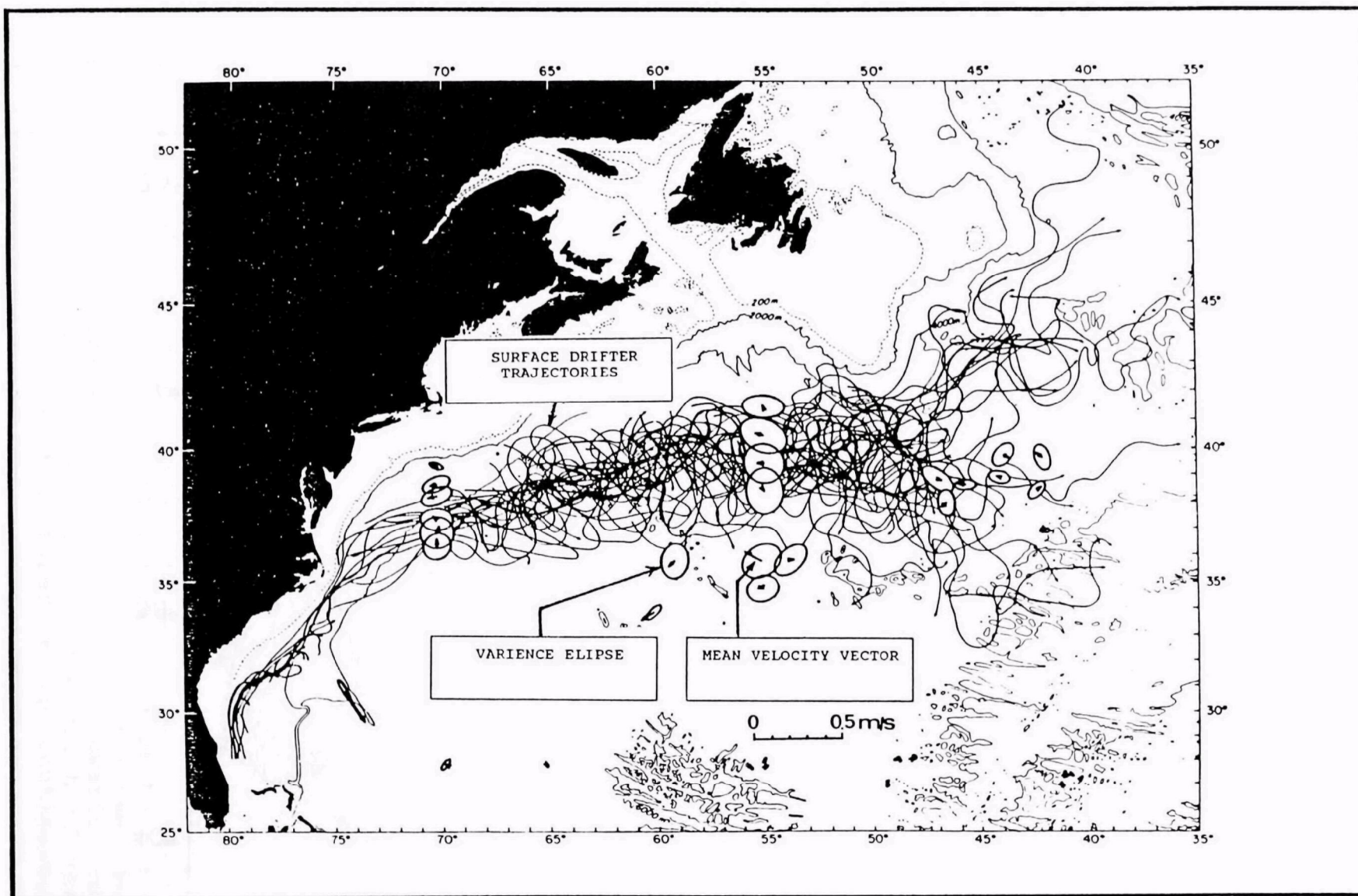


Figure 3-3. A comparison of mean velocities and variance ellipses at 4000 m for the western North Atlantic. The approximate position of the Gulf Stream is shown by surface drifter trajectories (Richardson, 1983). The ellipse axes are proportional to rms speeds and are drawn to the same scale as the mean velocity vectors (from Fofonoff and Hendry, 1985).

The major axis of these ellipses appear to align with the local isobaths.

In a number of these experiments, it has been suggested that there may be a relationship, possibly indirect, between GS meander motions and deep currents in the vicinity of the GS. There is some evidence that the formation and passage of warm-core rings in the slope sea can affect the energy levels of deeper currents. Louis et al., (1982) detected strong shoreward propagating topographic waves over the Scotian slope and rise. The current oscillations occurred in bursts of 4-5 cycles which indicated isolated deterministic forcing rather than a steady stochastic energy flux. Louis et al., (1982) also observed Rossby waves having baroclinic depth structures on the slope and upper rise and predominantly barotropic at the slope-rise junction. One of the events in the Scotian rise current meter array was related to the formation of a small warm-core eddy at the crest of a large GS meander due south of the moored array. The wave field was successfully modeled as being due to an isolated vortex by Louis and Smith (1982). A description of the kinematics and dynamics of a mature warm-core ring is provided by Joyce (1984). He shows that a large warm-core ring can induce perceptible warming as deep as 4000 m but the velocity structure is confined to the upper 1000 m. Similar kinds of changes in depth structure are also observed in the deep MASAR current records from the southern Mid-Atlantic Bight (SAIC, 1987).

IV. DATA ANALYSIS

4.1 Introduction

Motions on the lower continental rise are dominated by Topographic Rossby Waves (TRWs), which are ubiquitous on the continental rise and slope of the Mid-Atlantic Bight and have been reviewed above. The Hudson Canyon 3800-m low-level radioactive waste disposal site mooring is north of the mean historical position of the cold wall or surface temperature front of the GS at 70°W. However, for about two thirds of the two year mooring I deployment period the monthly mean position of the cold wall was north of mooring I (SAIC, 1987). The mooring was about 30' west of the position of the 4000-m Rise Array mooring (Luyten, 1977; Thompson, 1977) deployed for nine months in 1973 and about 15' west of the northern end of the Inverted Echo Sounder (IES) line G from 1983 through 1984 (Tracey and Watts, 1986).

A sketch of the Hudson Canyon bathymetry (Fig. 1-1), taken from Hanselman and Ryan (1983), with the four mooring deployment positions indicated, shows that the channel is about 3 km wide, steep sided with walls about 250 m high, and a relatively flat bottom. About 10 km southeast of the mooring site, the channel broadens and begins to merge into the abyssal plain at depths beyond 4000 m.

The first three deployments were on the eastern side of the channel. The fourth deployment was deliberately placed on the western side of the canyon (about 2 km west of the previous locations) so as to determine if there were any differences in flow characteristics, particularly mean currents, between the two sides of the channel. Thus an attempt was made to determine if there was a possibility of a residual circulation within the canyon consisting of northwestward flow on one side and return flow on the other side. This turns out not to be the case, and as discussed below, the four deployments may be treated as a single mooring at a site approximately in the middle of the channel.

4.2 Mean Currents

Mean currents, of approximately 3-5 cm sec⁻¹, at water depths shallower than 4000 m along 70°W have been associated with the edge of the WBUC (Thompson, 1977), but mean currents in water deeper than 4000 m measured by the rise array showed little consistent westward drift. In the historical compilation of mean currents, Figure 3-2, relatively uniform westward drift of a few cm sec⁻¹ was found on the upper part of the rise.

Mooring I had relatively strong along-isobath (southwestward) flow above the canyon of about 4 cm sec⁻¹ which

indicated that the site was within the WBUC. Table 4-1 shows the statistics for currents measured during the complete two year deployment. Mean velocity, in cm sec^{-1} , and temperature, in $^{\circ}\text{C}$, are listed for each instrument level, along with the variances (U' denotes the deviation of the U-component of velocity from $\langle U \rangle$), Reynolds stresses $\langle U'V' \rangle$, mean temperature fluxes $\langle U \rangle \langle T \rangle$ and $\langle V \rangle \langle T \rangle$, and eddy temperature fluxes $\langle U'T' \rangle$ and $\langle V'T' \rangle$, where angle brackets $\langle \rangle$ denote that the mean of the quantity between them is calculated. The data from levels I 1, I 3 and I 4 are broken into time segments due to instrument failures. A comparison of the mean currents at I 2 and I 5 shows that the I 2 mean flow is directed across the canyon, while the I 5 mean flow, near the bottom, is directed up the canyon as might be expected. Mean current speeds increase slightly with depth between I 2 and I 5, reaching a maximum at 100 m above the bottom at I 4. However, a comparison between the first and fourth I.1 deployments show that six-month means can vary considerably between periods; a reflection of long time scales present in TRW motions and indirect influences of the GS. The more westward position of deployment 4 seems to make no significant difference in the direction of mean flows compared to earlier deployments. It appears, therefore, that the mean flow is relatively uniform across the channel. No residual internal horizontal circulation, due to canyon topography, is apparent in these measurements.

The statistics in Table 4 - 1 also show that the lower 400 m of the water column, effectively the depth of the canyon, is virtually homogeneous. Only very small (differences of 0.02°C) vertical temperature gradients T' exist between I 2 and I 5. This substantial, bottom-mixed layer, with a larger temperature variance at I 1 than at I 2 and below, is apparently caused by localized mixing and strong currents interacting with the canyon topography. The maximum current speed observed was 62 cm sec^{-1} and westward in direction at I 4. It occurred during the first deployment (Fig. 4-1) on approximately Julian Day (JD) 195. This maximum speed is similar to data from a rise array at 4000m depth (Luyten, 1977).

4.3 Topographic Rossby Waves (TRWs)

Deep water flows on the continental rise are dominated by TRWs. Hogg (1981) showed that nearly barotropic Rossby waves tend to dominate in water depths greater than 4000 m and bottom-trapped TRWs are more prevalent on the middle and upper rises. Therefore, it is expected that TRWs will dominate low frequency motions at periods longer than the Rossby wave cut-off period given by $T = (Na)^{-1}$; where N is the Brunt-Vaisala frequency of the lower water column and a is the bottom slope. For the general topography of the lower rise, T is about 8-10 days. Thus, low frequency current fluctuations have characteristic time scales longer than 10 days.

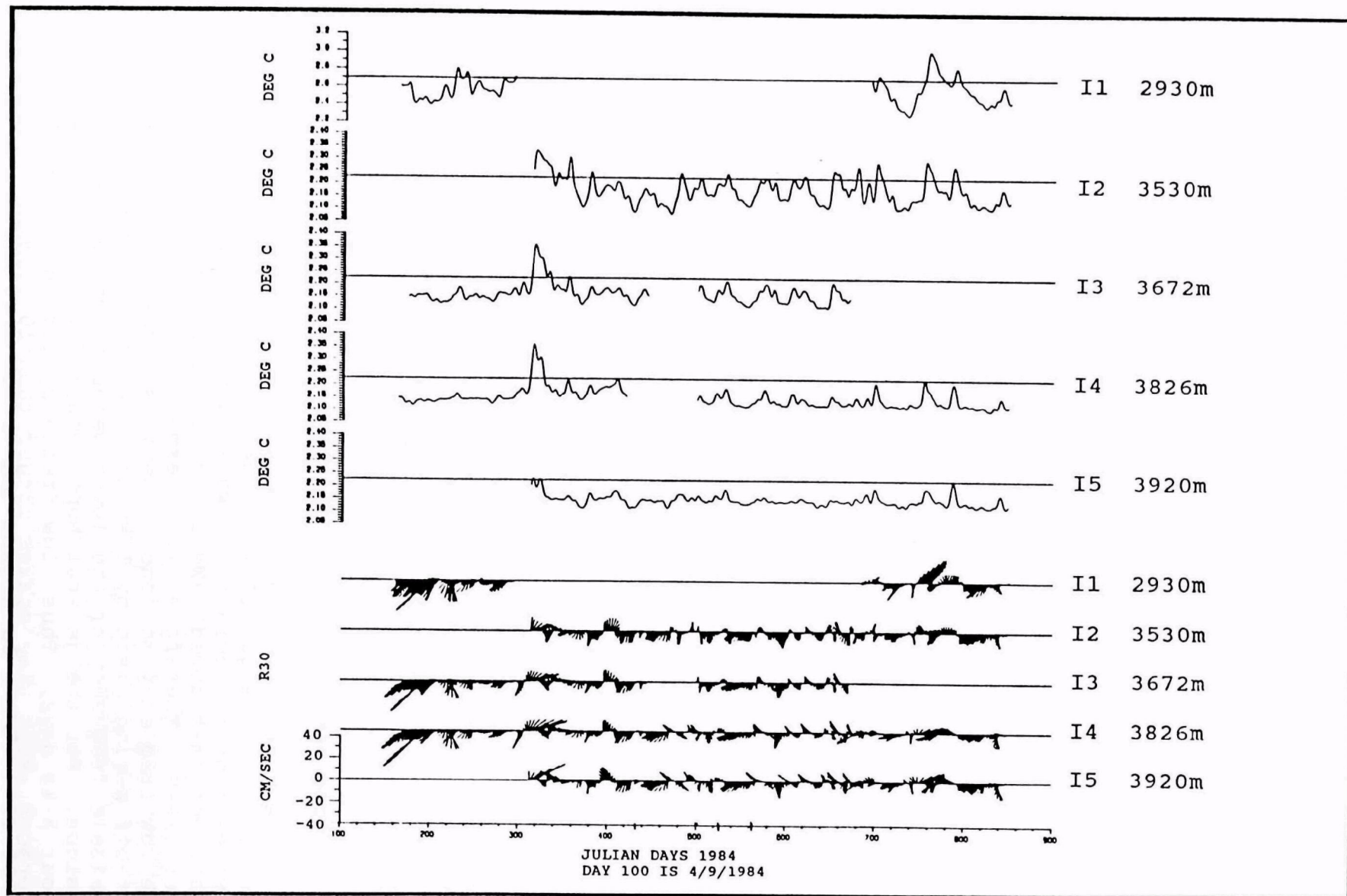


Figure 4-1. 7-DLP temperatures (top) and currents (bottom) by level on Mooring I. Note Current sticks are referenced to 030° true (vertical up position) in order to coincide with the orientation of isobaths Northeast and Southwest of the Hudson Canyon and are designated by R30 on the plots.

Important characteristics of TRWs are that the wave velocities are bottom intensified and columnar (i.e., no phase differences with depth). TRWs are discussed in more detail by Thompson (1977); Hogg (1981) and Hamilton (1984). The original theory is presented by Rhines (1970).

An important question addressed by the Hudson Canyon current data is the degree to which TRWs propagating westward, along the rise, influence the currents in a narrow channel cut into the seafloor; the channel having small dimensions compared with TRWs which have horizontal wavelengths on the order of 100-200 km and vertical scales of 2-3 km. The 7-DLP current data presented in Figure 4-1 and the 40-HLP currents and temperature data (Fig. 4-2 a-f) clearly show that the low-frequency motions penetrate all the way to the floor of the canyon, increasing in magnitude with depth. Occasional exceptions to this pattern are discussed below.

The main influence of the canyon on TRW motions seems to be an uncharacteristic relative rotation of current vectors with depth. This is shown more clearly by the principal axes calculations given in Table 4-1. The major and minor principal axes effectively give the direction in which the variance of the fluctuations is maximized and minimized, respectively. There is a counter clockwise rotation of the major axis of about 20° between I 1 and I 2 and a clockwise rotation of about 85° between I 2 and I 5. U-component variances dominate within the canyon, compared to almost equal U and V variances at I 1.

The time series current data plots (Fig. 4-2 a-f) show the high degree of coherence of both the currents and the temperature fluctuations through the water column. However, there is considerable variability in the energy levels of the fluctuations over the two-year period. The period from June to August, 1984 (JD 160-240) showed energetic, generally westward directed currents. It was also a period of large GS meanders and the formation of a warm-core ring (WCR 84-E) downstream (i.e. east) of the site. The month of June had a large southward displacement of the GS at about 69-68°W which formed a cold-core ring. This meander was present for most of June. A large warm-core ring began forming near 67°W with the GS displaced southward throughout the Mid-Atlantic Bight. The GS then interacts with newly formed WCR 84-E towards the end of July. This causes a reduction in size of the warm-core eddy which then propagates westward, reaching 70°W in the first part of September (JD 250). This is a period of relatively weak currents (approximately 10 cm sec⁻¹) at mooring I. At the end of September (JD 263) the GS shifted northward due to interaction with a cold-core ring (SAIC, 1987) east of Cape Hatteras. (JD 263). No strong westward currents occurred in the months of March-April, June and August 1985 when rings 84-G, 85-B and 85-F were near 70.5° W. Direct relationships between

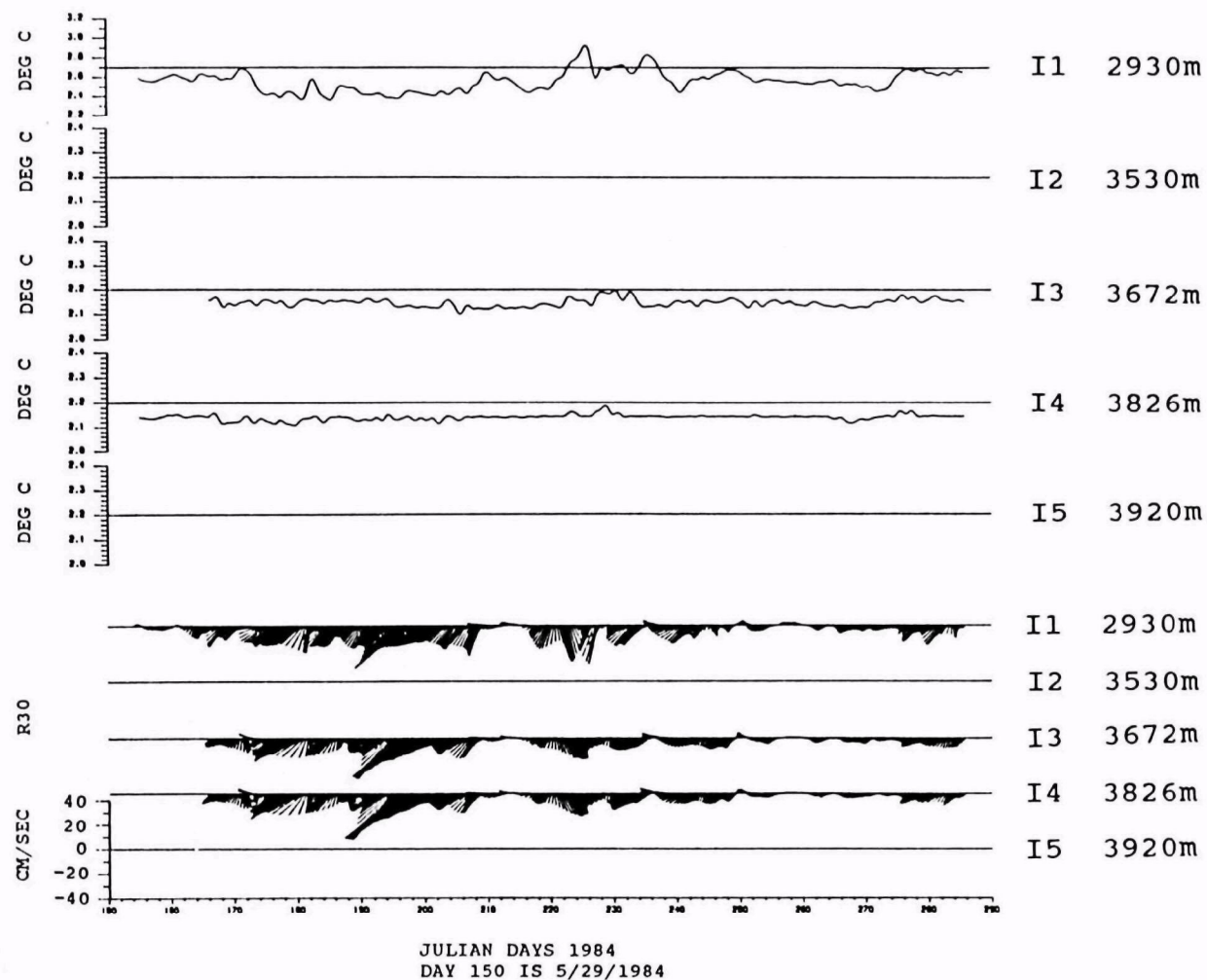


Figure 4-2a. Five month data record beginning May 29, 1984 of 40-HLP of temperatures (top) and currents (bottom) by level on Mooring I at the 3800-m low-level radioactive waste disposal site. Note Current sticks are referenced to 030° true (vertical up position) in order to coincide with the orientation of isobaths Northeast and Southwest of the Hudson Canyon and are designated by R30 on the plots.

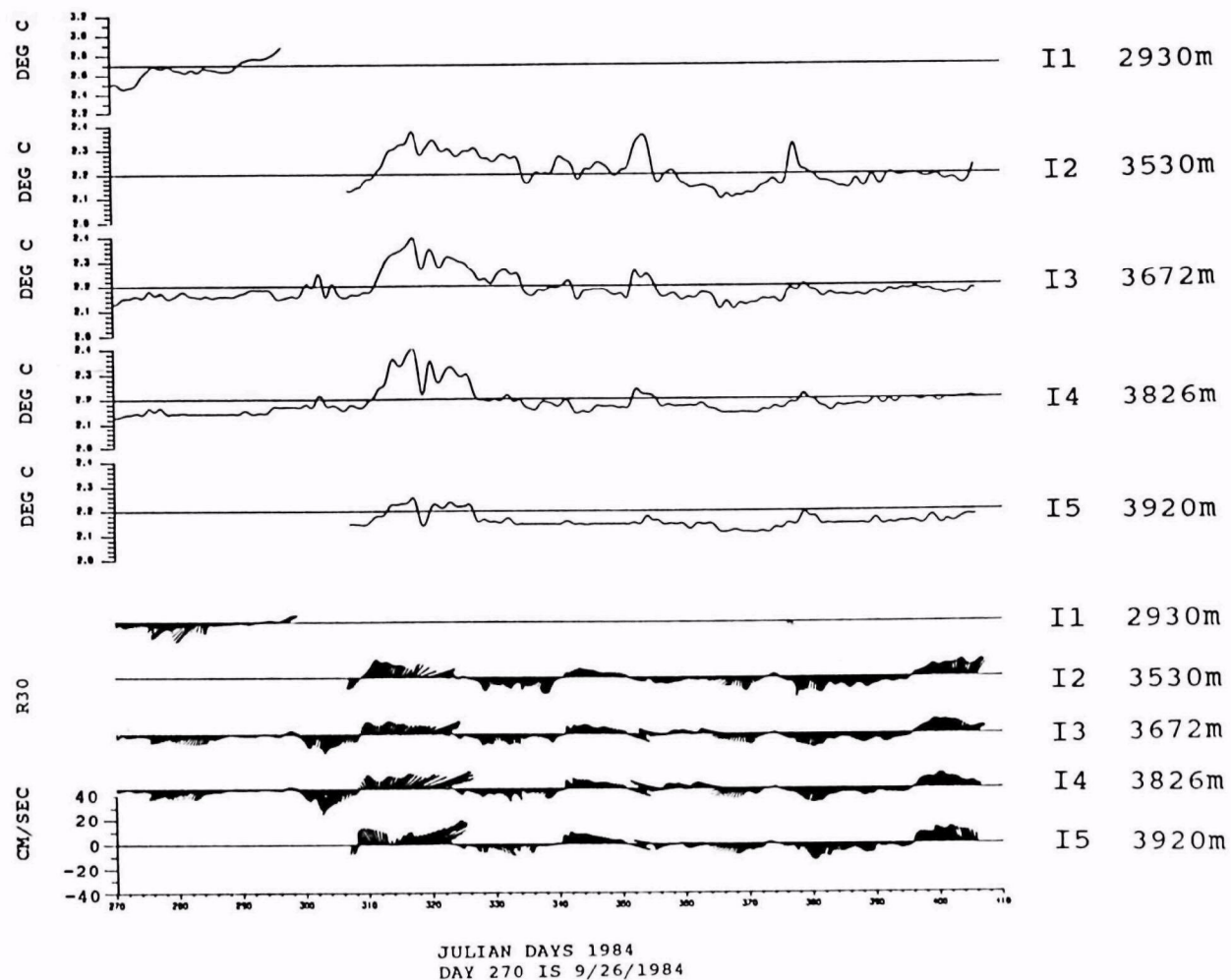


Figure 4-2b. Five month data record beginning September 26, 1984 of 40-HLP of temperatures (top) and currents (bottom) by level on Mooring I at the 3800-m low-level radioactive waste disposal site. Note Current sticks are referenced to 030° true (vertical up position) in order to coincide with the orientation of isobaths Northeast and Southwest of the Hudson Canyon and are designated by R30 on the plots. There is approximately a one month overlap from Figure 4-2a.

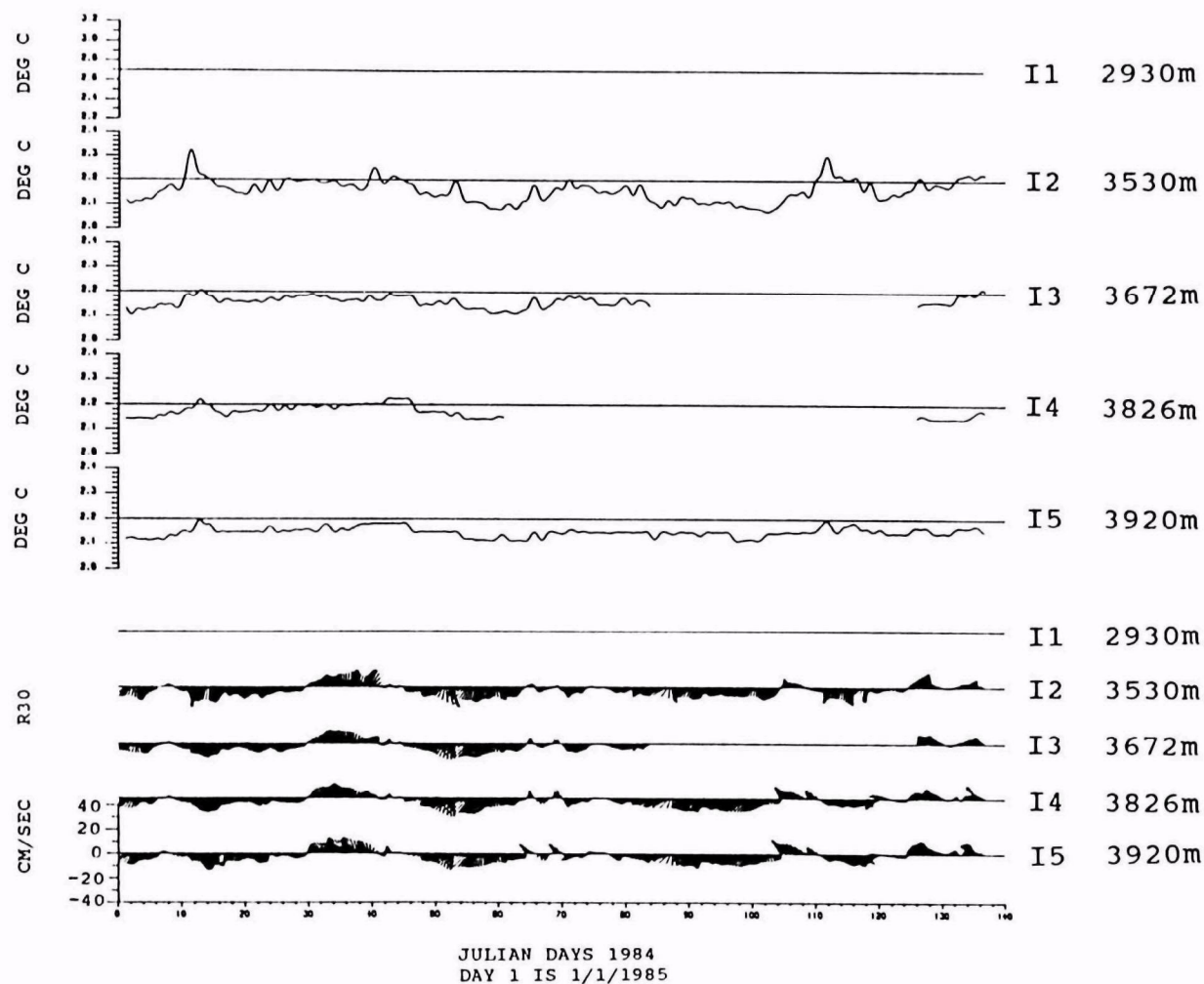


Figure 4-2c. Five month data record beginning January 1, 1985 of 40-HLP of temperatures (top) and currents (bottom) by level on Mooring I at the 3800-m low-level radioactive waste disposal site. Note Current sticks are referenced to 030° true (vertical up position) in order to coincide with the orientation of isobaths Northeast and Southwest of the Hudson Canyon and are designated by R30 on the plots. There is approximately a one month overlap from Figure 4-2b.

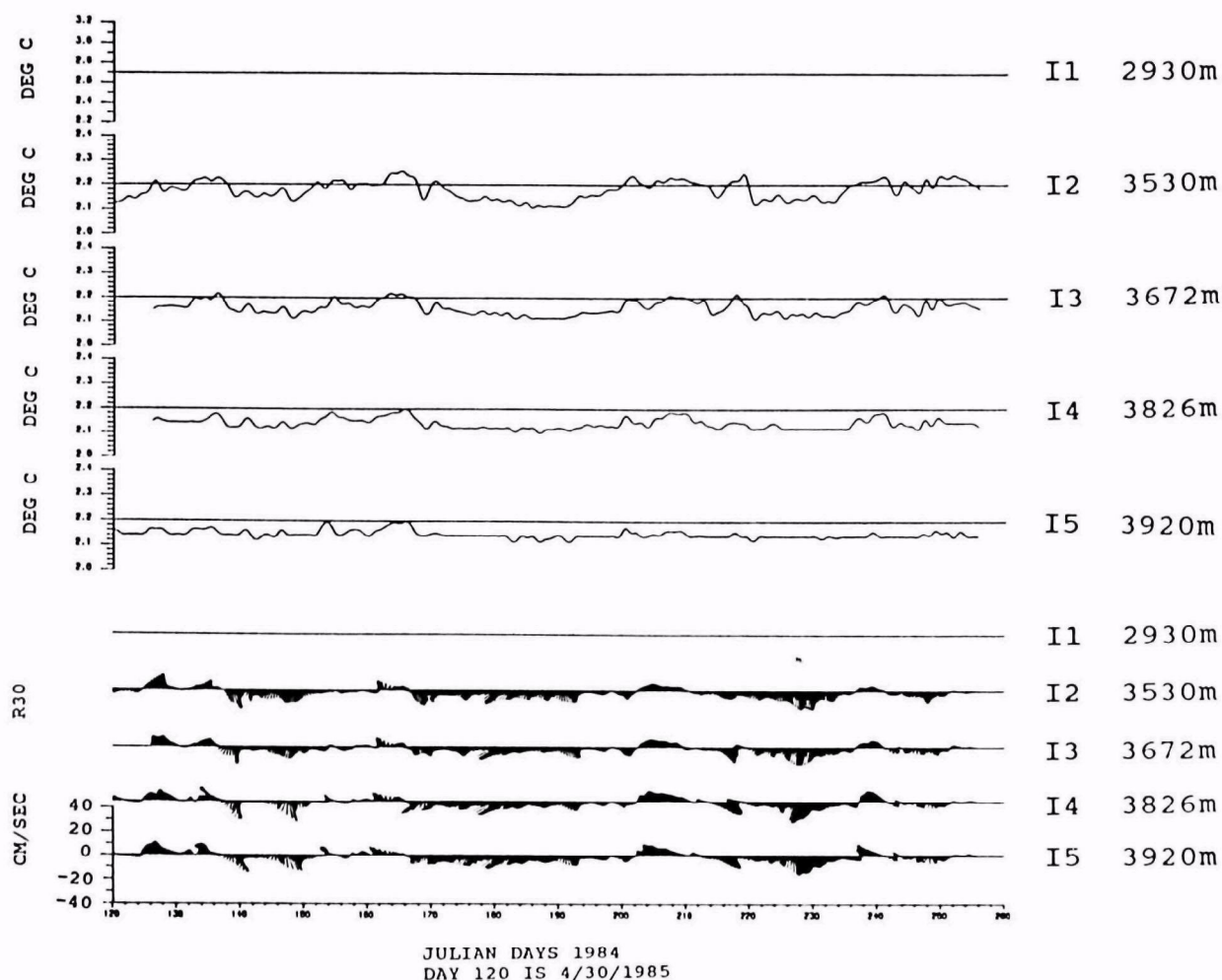


Figure 4-2d. Five month data record beginning April 30, 1985 of 40-HLP of temperatures (top) and currents (bottom) by level on Mooring I at the 3800-m low-level radioactive waste disposal site. Note Current sticks are referenced to 030° true (vertical up position) in order to coincide with the orientation of isobaths Northeast and Southwest of the Hudson Canyon and are designated by R30 on the plots. There is approximately a one month overlap from Figure 4-2c.

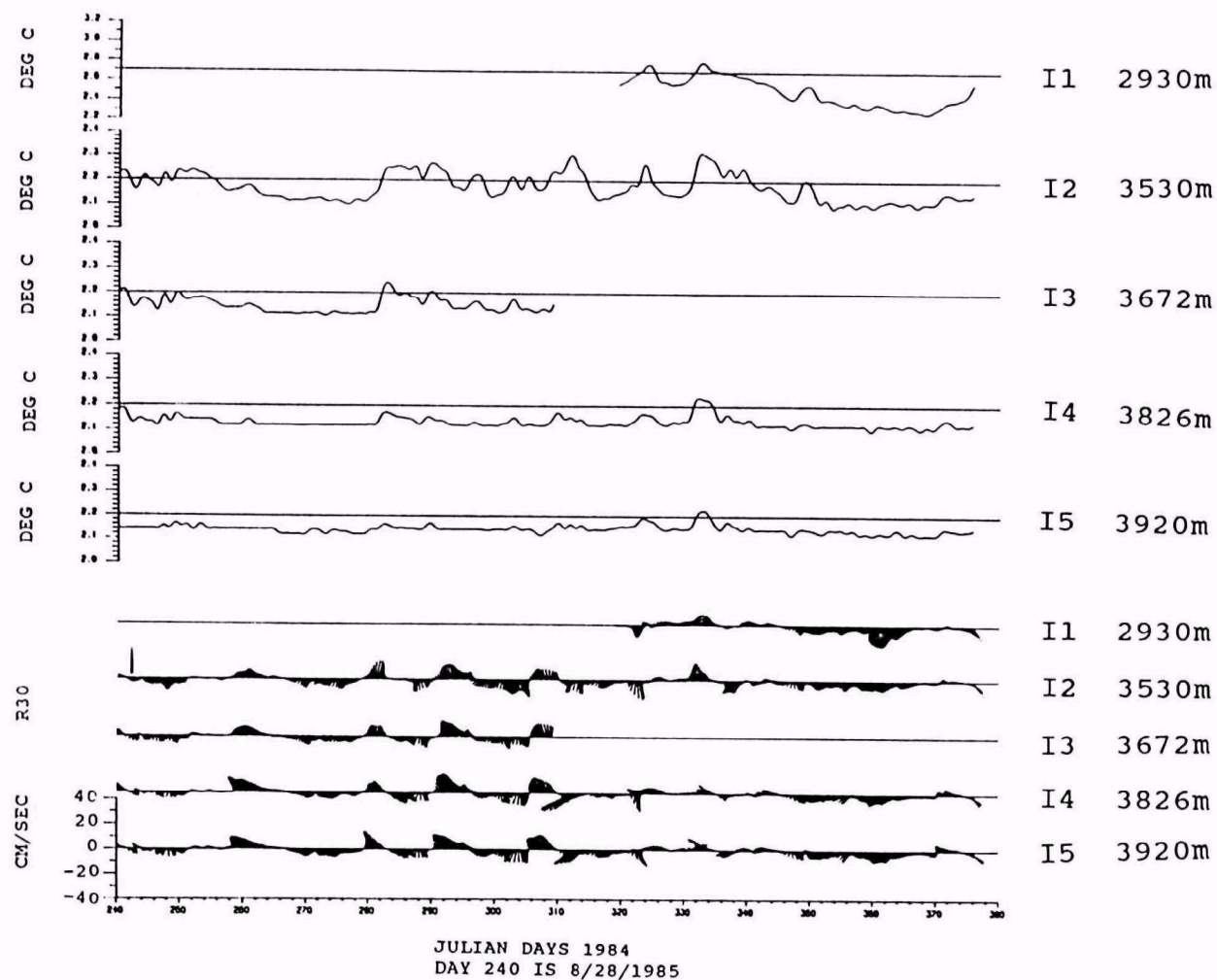


Figure 4-2e. Five month data record beginning August 28, 1985 of 40-HLP of temperatures (top) and currents (bottom) by level on Mooring I at the 3800-m low-level radioactive waste disposal site. Note Current sticks are referenced to 030° true (vertical up position) in order to coincide with the orientation of isobaths Northeast and Southwest of the Hudson Canyon and are designated by R30 on the plots. There is approximately a one month overlap from Figure 4-2d.

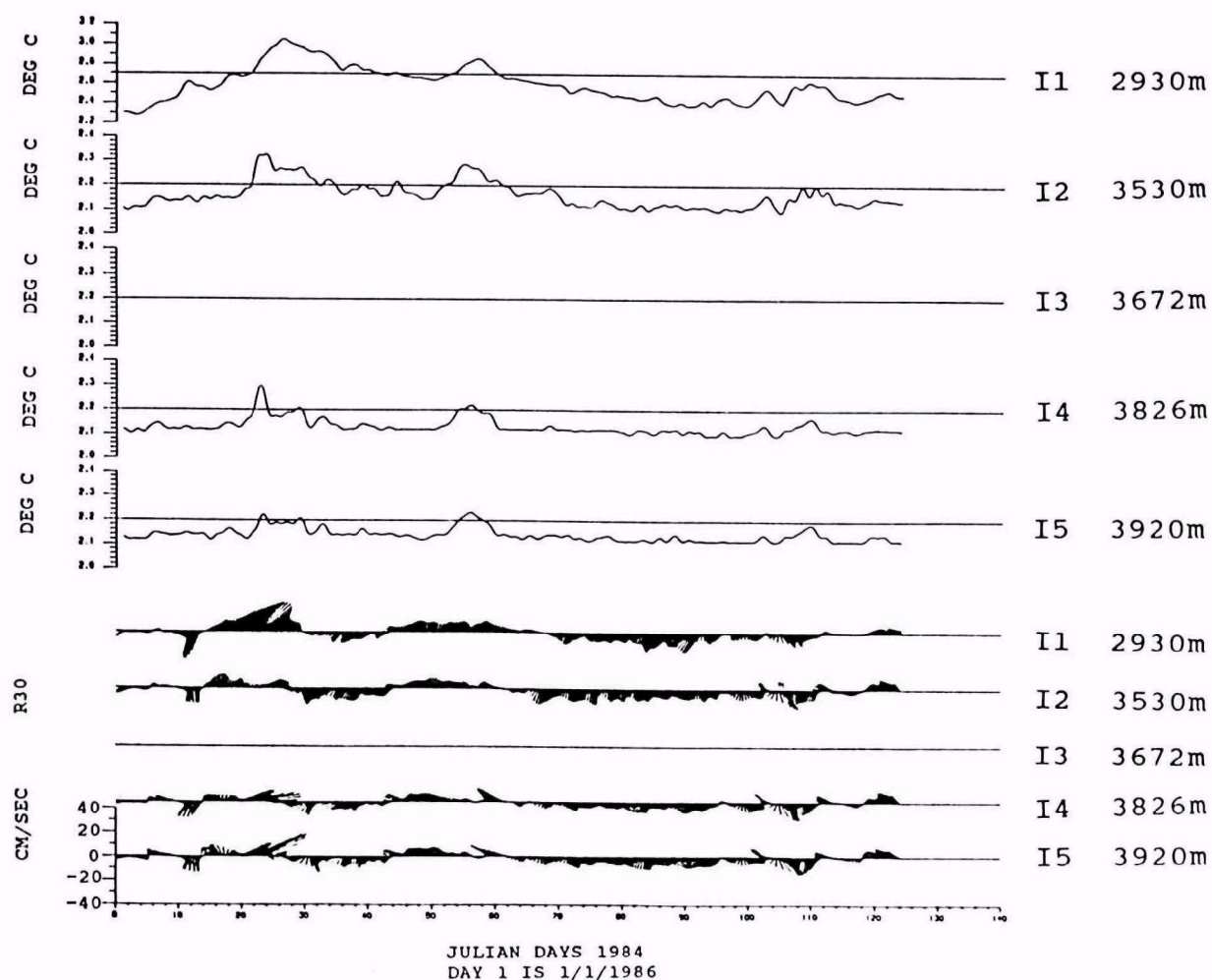
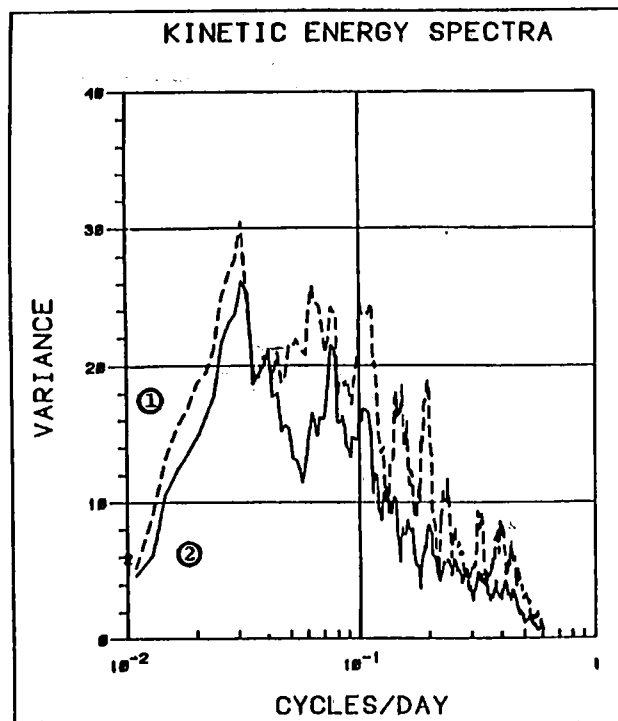


Figure 4-2f. Five month data record beginning January 1, 1986 of 40-HLP of temperatures (top) and currents (bottom) by level on Mooring I at the 3800-m low-level radioactive waste disposal site. Note Current sticks are referenced to 030° true (vertical up position) in order to coincide with the orientation of isobaths Northeast and Southwest of the Hudson Canyon and are designated by R30 on the plots. There is approximately a one month overlap from Figure 4-2e.

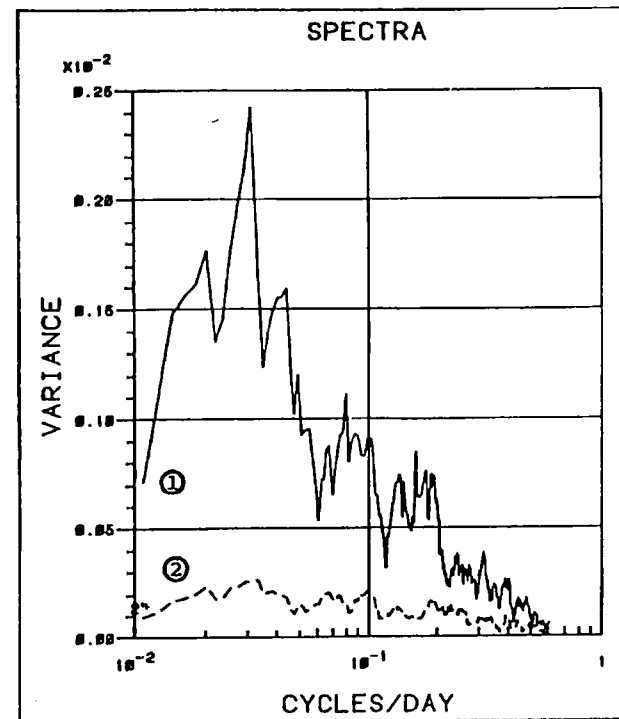
the position of the GS cold wall, the presence of rings, and the character of the flow on the lower rise are not obvious from these data, even though subtle connections involving the generation and propagations of TRWs and the GS are thought to be dynamically important.

Compared to the June to August, 1984 high current period, JDs 235-335, 1985 (days 600 - 700, Fig. 4-1) had relatively short period, weak fluctuations ($<10 \text{ cm sec}^{-1}$) exhibiting northward flow along the axis of the canyon. However, in contrast to these relatively low-energy periods, the last 5-month deployment showed a strong eastward event (JD 10-30, 1986; Fig. 4-2f) at I 1 which exceeds the velocities of the deeper instruments. A similar strong eastward event, accompanied by anticyclonic rotation of the current vectors and a sharp increase in temperature, occurred at the beginning of the second deployment at about JD 310, 1985 (Fig. 4-2b). Unfortunately, current measurements at I 1 were not obtained for this event. The unusual nature of these two strong eastward events along with the presence of warmer water may indicate a more direct influence of the deep GS, though this interpretation is speculative. Examination of the satellite imagery for these two dates show that on both occasions a GS meander crest is over the site and thus a direct GS effect on the flow may be a reasonable explanation of these events.

The kinetic energy spectra, in variance preserving form for I 2 and I 4, are shown in Figure 4-3. Variance preserving spectra plots give a better feel for the distribution of fluctuation energy or variance with frequency than conventional log-log spectra plots, since equal areas under the curve represent equal amounts of variance. The fluctuating kinetic energy is greater at I 4 than at I 2, at all frequencies along with a sharp decrease in energy at I 2 at about 0.15 cycles per day (cpd) which corresponds to the Rossby wave cut-off frequency. This increase in energy with depth is consistent with TRW dynamics despite the existence of the canyon. The 18-month time series used for these calculations resolves the major low frequency peaks at 0.03, 0.06 and 0.075 cpd, (33, 16 and 13 day periods, respectively). These frequencies have been associated with Rossby waves, and GS meanders in previous studies (Hogg, 1981). A feature of Figure 4-3 is the occurrence of spectral peaks at frequencies greater than the cut-off for currents within the canyon (I 4). These peaks occur at discrete frequencies which seem to be harmonics of major low-frequency peaks. An examination of the U and V component spectra ($> 0.15 \text{ cpd}$) (Fig. 4-4) shows that the higher frequency harmonics are more associated with the U than V component at I 4. The U component also shows increased variance with respect to the V component. Thus, the currents are being channelized and distorted within the canyon so that energy is transferred to the higher harmonics as the Rossby waves propagate over this feature. There is no visual indication from 40-HLP data (Fig. 4-2) that distinct wave motions associated with the channel (i.e., channel modes) are being set

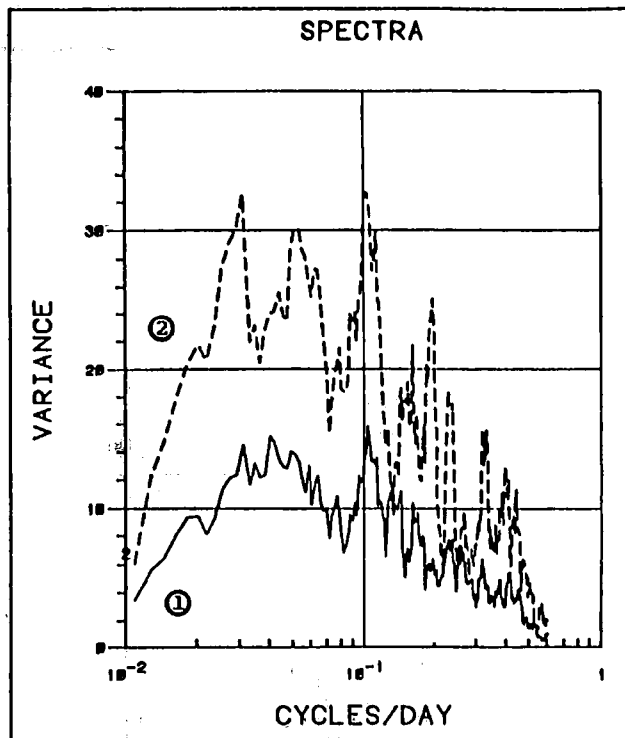


(a)

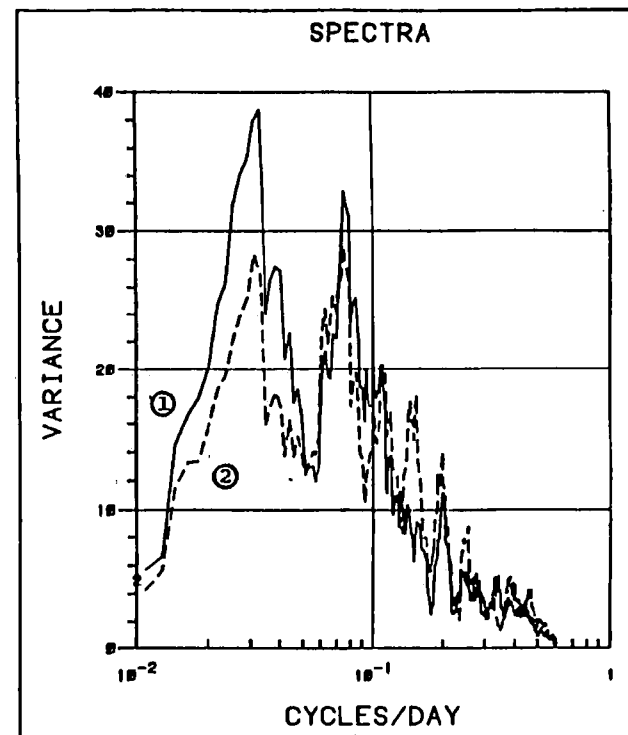


(b)

Figure 4-3. Spectra of (a) kinetic energy for levels I 2 (2-dashed) and I 4 (1-solid) and (b) temperature for instrument levels I 2 (1-solid) and I 5 (2-dashed). The time series length is 548 days beginning November 2, 1984.



(a)



(b)

Figure 4-4. Spectra of the (a) U component and (b) V component for I 2 (1 - solid) and I 4 or I 5 (2 - dashed). The time series length is 548 days beginning November 2, 1984.

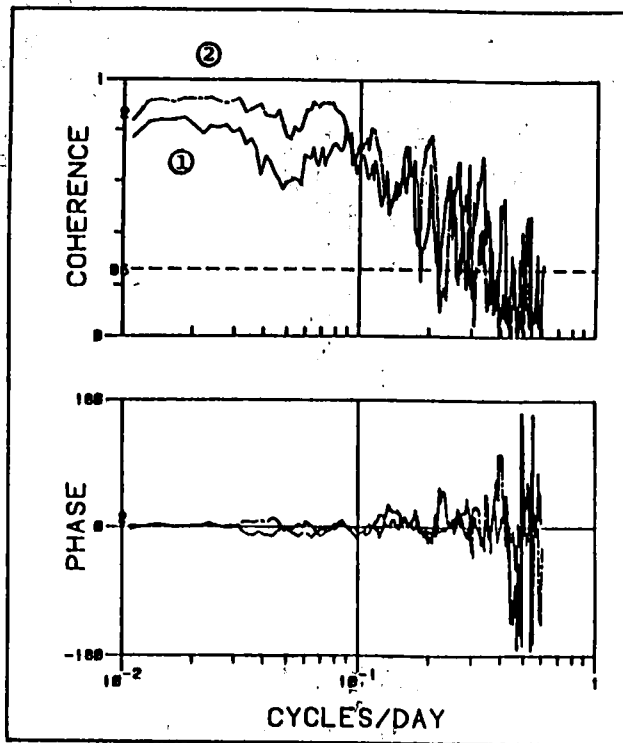
up at frequencies greater than 0.1 cpd. This artifact of spectral analysis is similar to the harmonics generated by the distortion of a semi-diurnal tidal wave propagating into a shoaling estuary.

Unlike the current velocity spectra, the temperature spectra show decreasing variance with increasing depth (Fig. 4-3). The current and temperature fluctuations at low frequencies are also highly coherent and in phase throughout the depth of the mooring (Fig. 4-5). Temperature and the U component of current are also correlated with velocity leading temperature by about 60° at all frequencies below 0.1 cpd (Fig. 4-6). Usually for TRWs, temperature and currents are in quadrature (i.e. 90° phase difference) since waves do not transport heat. However, in the case of waves in the canyon, there is a small, down-canyon flux of heat most clearly evident from the velocity and temperature records at I 3, I 4, and I 5. This implies that the distortion of the TRW wave motions by the canyon causes horizontal mixing of temperature or pollutants which causes a diffusive flux against the mean up-canyon currents.

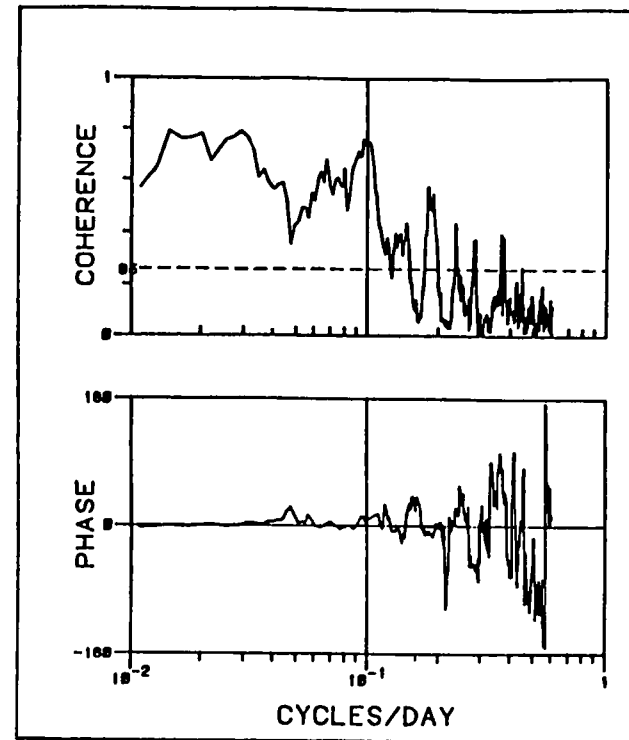
Table 4-1 contains the 40-HLP statistics for the longest combined records at each instrument. Of particular interest are the Reynolds Stresses $\langle U'V' \rangle$ and the mean and fluctuating components of the heat flux. The Reynolds Stress is quite variable with the four, six-month deployments, but above the canyon $\langle U'V' \rangle$ is positive, which is consistent with Rossby waves propagating westward and onshore. Within the canyon, the momentum flux can change sign. This seems to be the case for the relatively quiescent 1985 period (compare I 2 and I 5). However since the motions are essentially in phase between I 2 and I 5, the change in momentum flux must be related to the distortion of the wave motions by the canyon. Again the large variability in all the calculated statistics is noted even though the averaging period is six months to one year. The eddy fluxes are an order of magnitude smaller than the mean advective heat fluxes. The eddy fluxes oppose the advective fluxes. The T' variances and eddy fluxes at the upper level (I 1) exceed that of 2800-m dumpsite (Hamilton, 1984) and are comparable within the canyon indicating that the upslope and along slope temperature gradients are relatively substantial for the 4000-m depth, despite the 300-400 m deep bottom mixed layer.

4.4 Relationship to the Gulf Stream

The relationship between the Gulf Stream and deep current motions under and north of the stream is not straightforward. Further theoretical developments are needed before the mechanisms of GS meandering and birth of rings, which are thought to be the energy sources of deep Rossby wave motions, are better understood. The relationship of deep currents to the GS is quite subtle and only indirect connections can be suggested in this report.

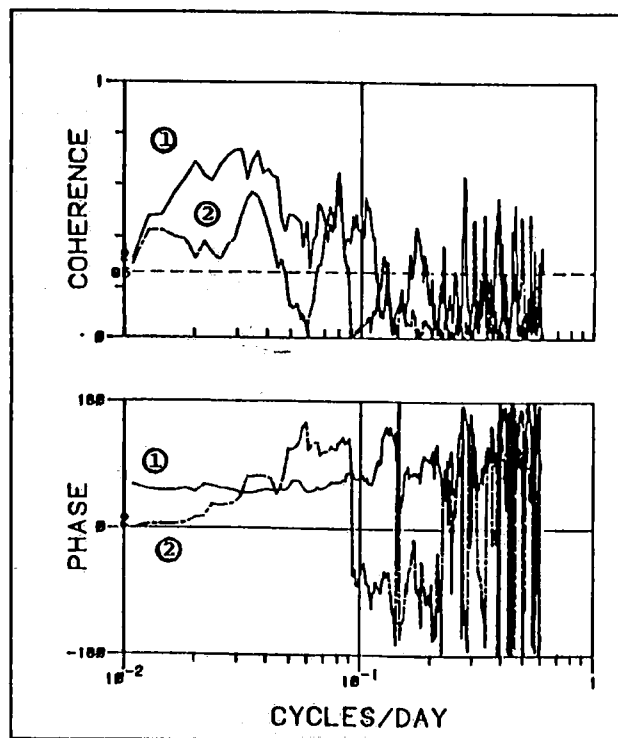


(a)

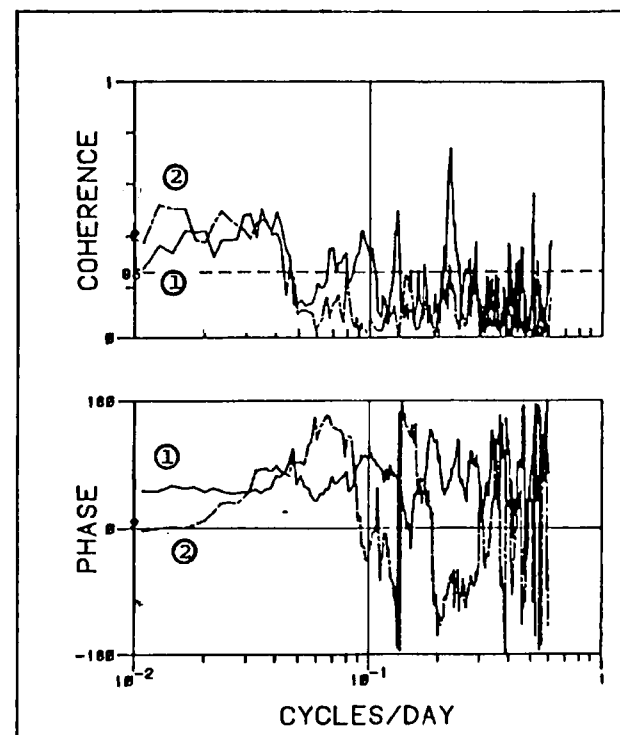


(b)

Figure 4-5. Coherence and phase differences between (a) the U components (1 - solid) and the V components (2 - dashed), with axes rotated 30° , of I 2 and I 4, and (b) the temperature at I 2 and I 4 or I 5. The time series length is 171 days beginning November 11, 1985.



(a)



(b)

Figure 4-6. Coherence and phase differences between the U (1 - solid) and V (2 - dashed) components, with axes rotated 30° , and temperature at level (a) I 2 and (b) I 5. The time series length is 548 days beginning November 2, 1984.

There is some evidence that the path of the GS influenced the TRW energy levels at mooring I and at MASAR sites D, E, G and H (SAIC, 1987). During the first four months of this study, the GS followed its usual path, leaving the slope at Cape Hatteras and remaining south of the 4000-m isobath at 70°W. This was also a period of intense meander activity and formation of a cold-core ring and a large warm-core ring, downstream of the site, between 70° and 65°W. Energy levels at mooring I were larger than in subsequent periods. Since TRWs propagate westward along the bathymetry (Hogg, 1981), it is likely that the formation of a large warm-core ring, which underwent an intense interaction with a GS meander in July 1984, was partly responsible for the increased wave energy. Between October 1984 and December 1985 (JD 270-720; Fig. 4-1) the GS was further north of its historical position (Figure 3-1). In fact, the GS front was often north of the 3800-m dumpsite during this period. TRW fluctuations were weaker and of higher frequency than the earlier period. Fewer large warm-core rings were generated in 1985 west of 65°W. The propagation of three rings into the Hudson Canyon region in the spring and summer of 1985 (84-G, 85-B and 85-F) appeared to have minimal effect, if any, on the currents at mooring I. No bursts of energetic, low frequency current fluctuations were observed. Meanders of the GS were also less frequent, between 70° and 65°W, during most of 1985.

From December 1985 to the end of this study in May 1986, TRW energy levels increased. The increase seems to correspond to the GS shifting back to a more normal path at the beginning of December. However, a very large southward meander occurred near 68°W during December with the possible formation of cold-core rings, similar to the meander and cold-core ring formation in June 1984. Thus it is not clear which event, the GS shift or the large meander, was responsible for the increased TRW activity.

Apart from TRWs, there appeared to be two events that could be related to the GS proper. Between JD 312 and 322 (1984) and between JD 14 and 30 (1986), see Figs. 4-2b and 4-2f, substantial eastward flows occurred. The down-canyon components were accompanied by relatively large increases in temperature. Imagery shows large meander crests moving over the site at both times. It seems reasonable to attribute both events to intermittent deep GS flow causing an acceleration in lower layer currents, as discussed by Shaw and Rossby (1984). This is substantiated in the second event since maximum velocities occurred at I 1 rather than near bottom, as is more usual for TRWs. The I 1 record was not available for the first event.

GS thermocline maps, derived from an IES array (Tracey and Watts, 1986), clearly show a large meander propagating eastward through the array between the middle

of September and the end of November 1984 (Tracey, Cronin and Watts, 1985). The crest arrives at the site 26-30 November, JD 270-275 about 20 days prior to the warm eastward flow event at mooring I. The GS remains in a northern position close to the slope for most of December. Thus, even though the correlation with GS meander crest events is not exact, the assumption that GS caused the eastward flow events at 4000 m seems possible.

4.5 Higher Frequency Motions

Near-inertial internal wave motions are generated primarily by changing wind forcing at the ocean surface such as due to the passage of storms and fronts. The waves propagate down below the wind-mixed layer in the form of clockwise horizontal rotating currents (looking down above) with a periodicity close to f , the Coriolis parameter. These motions are intermittent and thus the spectra has broad peak near f . U and V component amplitudes are almost equal, with V leading U by 90° consistent with a constant current vector rotating at a frequency near f . Inertial currents were shown to be the dominant higher frequency motions at the 2800-m dumpsite on the upper rise (Hamilton, 1984). Maximum speeds due to inertial oscillations approached 10 cm sec^{-1} on occasion with average amplitudes $3\text{-}4 \text{ cm sec}^{-1}$. The lower Hudson Canyon dumpsite is 1000 m deeper than the 2800-m site and since surface layer wind forcing is the source of inertial currents, it is expected that near-inertial internal waves would be more attenuated at the greater depth. Figures 4-7 a & b show the rotary spectra for I 1 and I 4 for the last six-month deployment period. Linear frequency axes have been used so as to emphasize the higher frequency inertial and tidal motions. At I 1, a fairly sharp inertial peak is observed in the clockwise rotating component at about 1.3 cpd. A semi-diurnal (M2) spectral peak is also present at 1.95 cpd. At I 4 both inertial and semi-diurnal tidal peaks have become broader. The M2 tide has similar energy to that at I 1 though the anticlockwise rotary component is attenuated. The inertial peak within the canyon is not as energetic as at I 1. The local inertial frequency, f , is 1.23 cpd for $37^\circ 50' \text{N}$ latitude. Thus, the inertial peak at I 1 is about 6% higher than f as is expected for propagating near-inertial internal waves.

Within the canyon however, the peak splits into two with the lower frequency peak being less than f (about 1.20 cpd). The reason for this are not clear, but the implication is that the mean flow field contains negative (cyclonic) relative vorticity which can support sub-inertial internal waves. The implication is that the mean currents have horizontal shear, possibly due to the frictional effects of the canyon walls (Mooers, 1975).

Figure 4-8a shows the kinetic energy spectra for the last deployment of I 1 plotted in variance preserving form, where equal areas under the curve represent equal amounts of variance.

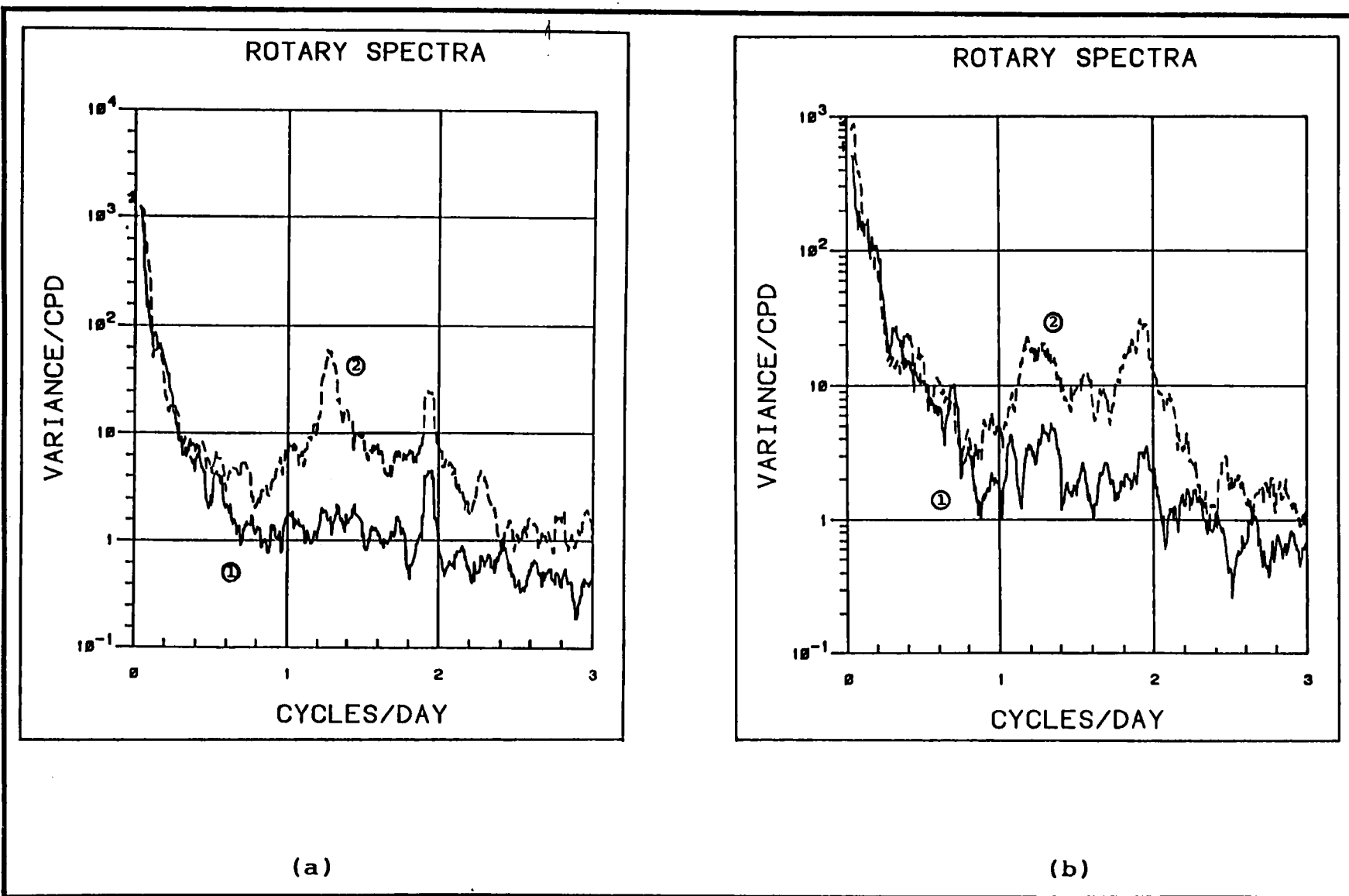
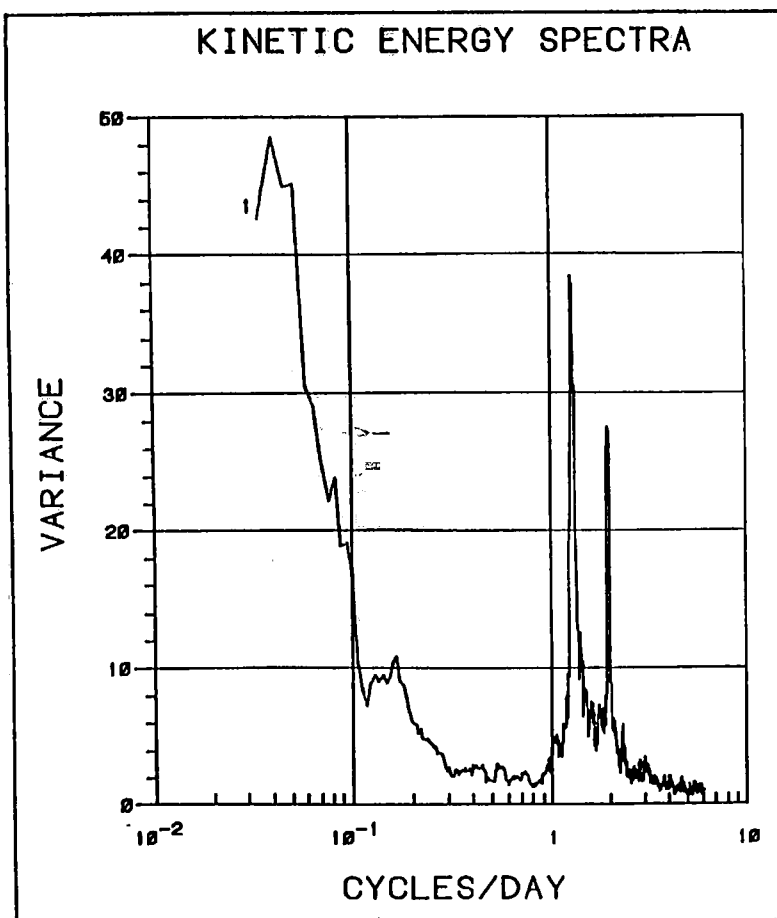
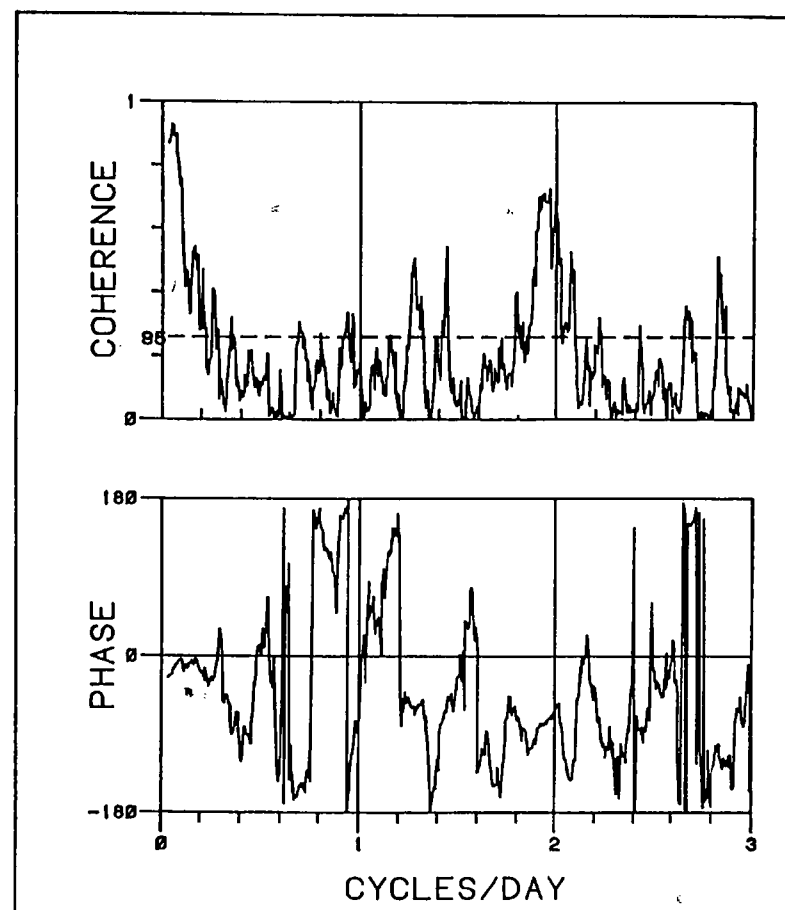


Figure 4-7. Rotary spectra for (a) I 1 clockwise component (1 - solid) and anticlockwise component (2 - dashed) and (b) I 4 clockwise component (1 - solid) and anticlockwise component (2 - dashed). The time series length is 171 days beginning November 11, 1985.



(a)



(b)

Figure 4-8. (a) Kinetic energy spectra plotted in variance preserving form for I 1 for 171 days beginning November 2, 1985. (b) Coherence of inertial and tidal motions for the clock wise rotary components at I 1 and I 4 for 171 days beginning November 2, 1985.

It can be seen that inertial and semi-diurnal tidal peaks are quite prominent at frequencies greater than 1 cpd but they account for only a small proportion of the total energy which is dominated by the low frequency TRW wave motions. The amplitude of the M2 tidal currents is approximately 1 cm sec^{-1} and the inertial currents $2\text{-}3 \text{ cm sec}^{-1}$. This downward propagating internal wave kinetic energy is expected to be dispersed by the canyon boundary layers and thus may contribute to mixing.

The coherence of inertial and tidal motions is shown in Figure 4-8b for the clockwise rotary components at I 1 and I 4. The tidal records show a high degree of coherence, the inertial currents less so. The phase propagation is vertically upwards at both frequencies as is expected for downward propagating internal wave packets. The 60° to 90° phase differences imply a vertical phase velocity of about 3 cm sec^{-1} which is comparable to the values calculated at the 2800-m dumpsite (Hamilton, 1984).

V. SUMMARY

The near-bottom current and temperature fields at the 3800-m low-level radioactive waste dump site have been investigated using data from a two-year-long mooring (May 1984-May 1986) deployed in the lower Hudson Canyon. Aanderaa current meters were nominally placed at about 5, 100, 250, 400, and 1000 m off the bottom. The upper two instruments were above the lip of the canyon, the middle instrument approximately at the canyon lip and the lower two instruments within the canyon.

The dominant motions were low frequency topographic Rossby waves with characteristic periods of 33, 16, and 13 days. Two-year-long records were needed to resolve the energetic longer period motions. The wave motions were generally bottom intensified, columnar, and penetrated to the floor of the canyon. The effect of the canyon primarily was to distort the essentially linear waves below the lip, introducing some non-linearity which introduced spectral peaks at frequencies higher than the Rossby wave cut-off (about 8 days). The average kinetic energy of the Rossby wave motions varied by more than a factor of two with deployment period and seemed to have a subtle relationship to the position of the Gulf Stream. When the GS was north of its historical mean position during most of 1985, energy levels were approximately 40-50% lower than in either 1984 or 1986 when the GS followed its more normal path after leaving Cape Hatteras. However, the higher energy levels were also associated with higher degrees of GS meander activity downstream of the site. There were two strong eastward flow events accompanied by warmer water that may be associated with GS meander crests overlying the site and could be examples of the intermittent deep GS flows that have been observed with SOFAR floats (Shaw and Rossby, 1984).

Mean currents above the canyon for the two-year period were substantial (approximately 3.5 cm sec^{-1} at 230° True (T) at 400 m from the bottom) and directed to the west. Within the canyon, mean flows (approximately 5 cm sec^{-1} at 100 m from the bottom) tended to be directed more upslope (approximately 240° T) and there was no evidence of any residual circulation internal to the channel. The westward mean flows suggest that the site is on the southern edge of Western Boundary Undercurrent (WBUC). Mean temperatures were essentially uniform throughout the lower 400 m of the water column, implying that the interaction of the Rossby waves with the canyon topography generate enough mixing to homogenize the density structure.

Higher frequency motions are weak and consist of near-inertial and semi-diurnal internal waves with amplitudes of 2-3 and 1 cm sec^{-1} , respectively.

The implications for disposal of pollutants is as follows. Pollutants dissolved in the water should be subject to a mixing through the boundary layer which is greater than the depth

of the canyon. Maximum current speeds measured at 5 m and 100 m from the bottom are 45 cm sec^{-1} and 62 cm sec^{-1} , respectively. Mean flows tend to be up the canyon towards the upper slope within the canyon and westward above the canyon. Therefore, whether a constituent is mixed above the canyon lip or remains within the canyon, it will eventually end up in the WBUC and be transported westward towards Cape Hatteras, similar to the fate of dissolved constituents at the 2800-m site on the upper rise.

During the two-year study, there were two strong (approximately 50 cm sec^{-1}) eastward events which have been attributed to the Gulf Stream. Such flows would transport pollutants eastward (i.e. down-canyon) towards deeper water. The deep Gulf Stream is an intermittent feature and thus water particle trajectories, once out of the Gulf Stream are likely to return northwards to the WBUC.

Once dissolved, pollutants reaching the Cape Hatteras region via the WBUC, could be entrained into the deep GS which is more prevalent there (Watts and Johns, 1982) and then returned back to the WBUC downstream or further east. Alternatively, they could remain within the WBUC and continue southwards towards the South Atlantic. Water mass analyses implemented with some current meter data have traced the WBUC, from its formation by Denmark Strait overflow, to as far south as the continental slope off the Bahamas (Fine and Molinari, 1987).

Particulate matter, if sufficiently fine grained, has a greater propensity for sediment transport, due to the stronger maximum currents observed, in the lower Hudson Canyon than at the 2800-m site (60 cm sec^{-1} versus 40 cm sec^{-1}). Maximum near bottom flows were directed both up-and down-channel but with the strongest event (JD 180-200, 1984) being directed up-channel. Therefore, the long period fluctuations of the Rossby waves combined with the mean currents near the canyon bottom would move fine-grain sediments towards shallower water. Since Rossby wave current amplitudes decrease towards the slope region, the net result is probably deposition of any sediment possibly contaminated with radionuclides in shallower water to the northwest of the site. Whether sediment particles would leave the canyon and make it to the middle continental rise (approximately 3000-m depth) would require some model calculations to provide guidance. The occasional deep GS event also has enough energy to transport sediment eastward into deeper water.

Table 4-1

40-M.P Statistics for EPA Mooring I
Coordinate Axis Rotated 030°T

Meter	Period	$\langle U \rangle$ cm sec ⁻¹	$\langle V \rangle$ cm sec ⁻¹	$\langle T \rangle$ °C	$\langle U'^2 \rangle$	$\langle V'^2 \rangle$	$\langle U'V' \rangle$	$\langle U \rangle \langle T \rangle$	$\langle V \rangle \langle T \rangle$	$\langle T'^2 \rangle$	$\langle U'T' \rangle$	$\langle V'T' \rangle$
11	6/14/ to 10/23/84	-8.12	-8.86	2.57	56.81	65.37	29.58	-20.87	-22.77	0.0139	0.451	0.400
11	11/15/85 to 5/4/86	-1.67	-1.23	2.58	46.92	53.87	35.42	-4.31	-3.17	0.0276	0.505	0.616
12	11/2/84 to 5/4/86	-1.57	-3.14	2.17	23.54	37.60	4.10	-3.41	-6.81	0.00293	0.0975	0.0955
13	6/14/86 to 3/25/85	-4.24	-4.57	2.17	73.22	44.99	23.79	-9.18	-9.92	0.00198	0.188	0.090
13	5/6/ to 11/5/85	-1.91	-2.35	2.15	17.70	30.08	-2.46	-4.11	-5.05	0.00088	0.031	0.048
14	6/14/84 to 3/01/85	-5.31	-4.82	2.17	104.60	59.59	38.03	-11.52	-10.46	0.0020	0.257	0.151
14	5/6/85 to 5/4/86	-3.64	-1.67	2.14	40.84	31.36	-0.24	-7.79	-3.57	0.00062	0.055	0.035
15	11/2/84 to 5/4/86	-3.44	-2.05	2.15	47.33	39.33	-4.21	-7.40	-4.41	0.00049	0.047	0.036

VI. REFERENCES

- Aikman, F., H-W, Ou and R.W. Houghton, 1987. Current Variability Across the New England Continental Shelf and Slope. Submitted to Continental Shelf Research.
- Bower, A.S., H.T. Rossby, and J.L. Lillibridge, 1985. The Gulf Stream--Barrier or blender? J. Phys. Oceanogr., 15, 24-32.
- Cornillon, P., 1986. The Effect of the New England Seamounts on Gulf Stream Meandering as Observed from Satellite IR Imagery. J. Phys. Oceanogr. 16, 386-389.
- Fofonoff, N.P., and R.M. Hendry, 1985. Current Variability near the Southeast Newfoundland Ridge. J. Phys. Oceanogr., 15, 963-984.
- Fu, L-L., J. Vazquez and M.E. Parke, 1987. Seasonal Variability of the Gulf Stream from Satellite Altimetry. J. Geophys. Res., 92(C1), 749-754.
- Hamilton, P., 1984. Topographic and Inertial Waves on the Continental Rise of the Mid-Atlantic Bight. J. Geophys. Res., 89(C1), 695-710.
- Hamilton, P., 1982. Analysis of current meter records at the northwest Atlantic 2800 meter radioactive dumpsite, EPA Tech. Rep. 521/1-82-002.
- Halliwel, G.R., Jr., and C.N.K. Mooers, 1983. Meanders of the Gulf Stream downstream from Cape Hatteras 1975-1978. J. Phys. Oceanogr., 13, 1275-1292.
- Hendry, R.M., 1982. On the structure of the deep Gulf Stream. J. Mar. Res., 40, 119-142.
- Hogg, N.G., 1981. Topographic waves along 70°W on the continental rise. J. Mar. Res. 39: 627-649.
- Joyce, T.M., 1984. Velocity and Hydrographic Structure of a Gulf Stream Warm-Core Ring. J. Phys. Oceanogr., 14, 936-947.
- Louis, J.P., B.D. Petrie and P.C. Smith, 1982. Observations of Topographic Rossby Waves on the Continental Margin off Nova Scotia. J. Phys. Oceanogr. 12, 47-55.
- Louis, J.P., and P.C. Smith 1982. The Development of the Barotropic Radiation Field of an Eddy Over a Slope. J. Phys. Oceanogr., 12, 56-73.

- Luyten, J.R., 1977. Scales of motion in the deep Gulf Stream and across the continental rise. *J. Mar. Res.*, 35, 49-74.
- Mooers, C.N.K., 1975. Several effects of a baroclinic current on the cross-stream propagation of inertial-internal waves. *Geophys. Fluid Dyn.*, 6, 245-275, 1975.
- Owens, W.B., J.R. Luyten and H.L. Bryden, 1982. Moored velocity measurements on the edge of the Gulf Stream recirculation. *J. Mar. Res.*, 40(Suppl.), 509-524.
- Owens, W.B., 1984. A synoptic and statistical description of the Gulf Stream and subtropical gyre using SOFAR floats. *J. Phys. Oceanogr.*, 14, 104-113.
- Rhines, P.B., 1970. Edge-, bottom-, and Rossby waves in a rotating stratified fluid. *Geophysical Fluid Dynamics*. 1: 273-302.
- Richardson, P.S., 1977. On the crossover between the Gulf Stream and the Western Boundary Undercurrent. *Deep-Sea Res.* 24:139-159.
- Richardson, P.L., 1983. Eddy kinetic energy in the North Atlantic from surface drifters. *J. Geophys. Res.*, 88, 4355-4367.
- Richardson, P.L., J.F. Price, W.B. Owens, W.J. Schmitz, H.T. Rossby, A.M. Bradley, J.R. Valdes and D.C. Webb, 1981. North Atlantic subtropical gyre: SOFAR floats tracked by moored listening stations. *Science* 213, 435-437.
- Richardson, P.L., 1983. Eddy kinetic energy in the North Atlantic from surface drifters. *J. Geophys. Res.*, 88, 4355-4367.
- Rossby, T., E.R. Levine, and D.N. Conners, 1985. The isopycnal Swallow float--A simple device for tracking water parcels in the ocean. *Progress in Oceanography*, Vol. 14, Pergamon, 511-525.
- Rossby, T., A.S. Bower, and P-T Shaw, 1985a. Particle Pathways in the Gulf Stream. *Bull. Amer. Met. Soc.* 66(9), 1106-1110.
- Science Applications International Corporation, 1987. Study of Physical Processes on the U.S. Mid-Atlantic Continental Slope and Rise. Final Report, U.S. Dept. of Interior, Minerals Management Service, SAIC Report No. 86/7539.
- Schmitz, W.J., Jr., 1976. Eddy kinetic energy in the deep western North Atlantic. *J. Geophys. Res.* 81, 4981-4982.

- Schmitz, W.J., Jr., 1980. Weakly depth-dependent segments of the North Atlantic circulation. *J. Mar. Res.*, 38, 111-133.
- Schmitz, W.J., Jr., J.F. Price, P.L. Richardson, W.B. Owens, D.C. Webb, R.E. Cheney and H.T. Rossby, 1981. A preliminary exploration of the Gulf Stream system with SOFAR floats. *J. Phys. Oceanogr.*, 11, 1194-1204.
- Shaw, P-T, and H.T. Rossby, 1984. Towards a Lagrangian description of the Gulf Stream. *J. Phys. Oceanogr.*, 14, 528-540.
- Thompson, R.O.R.Y., 1977. Observations of Rossby waves near site D. *Prog. Oceanogr.*, 7, 135-162.
- Tracey, K.L., and D.R. Watts, 1986. On Gulf Stream meander characteristics near Cape Hatteras. *J. Geophys. Res.*, 91, 7587-7602.
- Tracey, K.L., M. Cronin, and D.R. Watts, 1985. The Gulf Stream Experiment: Inverted Echo Sounder Data Report for the June 1984 to May 1985 Deployment Period. University of Rhode Island, Narragansett, RI. GSO Tech. Rept. No. 85-3.
- Watts, D.R., and W.E. Johns, 1982. Gulf Stream meanders. *J. Geophys. Res.*, 87, 9467-9476.

ACKNOWLEDGMENTS

Sincere appreciation is expressed to Dr. Robert W. Houghton and the Lamont-Doherty Geological Observatory (LDGO), of Columbia University, for the loan of five Aanderraa RCM-5 current meters. The LDGO meters were a newer-designed version of the RCM-5 meters, specifically adapted for extended deployment in the deep ocean environment. The overall success of this two-year study is directly attributable to using the current meters provided by LDGO.

Sincere thanks are also expressed to Dr. James Lane of the Minerals Management Service (MMS), Department of the Interior. The two-year current measurement study, detailed in this report, was part of a broader MMS study of physical oceanographic processes along the U.S. mid-Atlantic slope and rise provinces. In his role as the overall MMS project manager, Dr. Lane provided frequent and able coordination support and assistance to the EPA project officer.